

Decoupling supernova and neutrino oscillation physics with LAr TPC detectors

I. Gil-Botella¹ and A. Rubbia²

Institut für Teilchenphysik, ETHZ, CH-8093 Zürich, Switzerland

Abstract

Core collapse supernovae are a huge source of all flavor neutrinos. The flavor composition, energy spectrum and time structure of the neutrino burst from a galactic supernova can provide information about the explosion mechanism and the mechanisms of proto neutron star cooling. Such data can also give information about the intrinsic properties of the neutrino such as flavor oscillations. One important question is to understand to which extent can the supernova and the neutrino physics be decoupled in the observation of a single supernova. On one hand, the understanding of the supernova explosion mechanism is still plagued by uncertainties which have an impact on the precision with which one can predict time, energy and flavor-dependent neutrino fluxes. On the other hand, the neutrino mixing properties are not fully known, since the type of mass hierarchy and the value of the θ_{13} angle are unknown, and in fact large uncertainty still exists on the prediction of the actual effect of neutrino oscillations in the event of a supernova explosion. In this paper we discuss the possibility to probe the neutrino mixing angle θ_{13} and the type of mass hierarchy from the detection of supernova neutrinos with a liquid argon TPC detector. Moreover, describing the supernova neutrino emission by a set of five parameters (average energy of the different neutrino flavors, their relative luminosity and the total supernova binding energy), we quantitatively study how it is possible to constrain these parameters. A characteristic feature of the liquid argon TPC is the accessibility to four independent detection channels ((1) elastic scattering off electrons, (2) charged neutrino and (3) antineutrino and (4) neutral currents on argon nuclei) which have different sensitivities to electron-neutrino, anti-electron-neutrino and other neutrino flavors (muon and tau (anti)neutrinos). This allows to over-constrain the five supernova and the flavor mixing parameters and to some extent disentangle neutrino from supernova physics. Numerically, we find that a very massive liquid argon detector (O(100 kton)) is needed to perform accurate measurements of these parameters, specially in supernova scenarios where the average energies of electron and non-electron neutrinos are similar (almost degenerate neutrinos) or if no information about the θ_{13} mixing angle and type of mass hierarchy is available.

Keywords: neutrino experiments, supernova neutrinos, liquid argon, TPC

¹Ines.Gil.Botella@cern.ch

²Andre.Rubbia@cern.ch

1 Introduction

Core collapse supernovae are a huge source of all flavor neutrinos. Neutrino astrophysics entered a new phase with the detection of neutrinos from the supernova SN1987A in the Large Magellanic Cloud by the Kamiokande and IMB detectors [1]. In spite of these fundamental neutrino observations, the 19 events observed are not statistically significant enough to obtain precise quantitative information on the neutrino spectrum. Currently running neutrino detectors like Superkamiokande [2] or SNO [3] have the capabilities to provide high statistics information about supernova and neutrino properties if a supernova collapse were to take place in the near future.

The flavor composition, energy spectrum and time structure of the neutrino burst from a galactic supernova can give information about the explosion mechanism and the mechanisms of proto neutron star cooling.

The neutrino signal from a galactic supernova can also give information about the flavor oscillation of neutrinos. Although new data from solar, atmospheric, reactor and accelerator neutrinos [4] have contributed to the understanding of the neutrino properties, still the neutrino mixing angle θ_{13} and the nature of the mass hierarchy, i.e., normal or inverted, remain unknown. Only an upper limit on the mixing angle is available dominated by negative measurements from reactor experiments [5]. These parameters can be probed by the observation of supernovae neutrino bursts, since neutrinos will travel long distances before reaching the Earth and will, as they travel through the exploding star, in addition traverse regions of different matter densities where matter enhanced oscillations [6] will take place. In the case of the θ_{13} angle, matter enhancement has the striking feature that very small mixing angles, beyond any value detectable by next generation accelerators, could in fact alter significantly the neutrino spectrum. Hence, supernova neutrinos provide indeed a complementary tool to study the θ_{13} angle.

The main question of course is to understand to which extent can the supernova and the neutrino physics be decoupled in the observation of a single supernova. On one hand, the understanding of the supernova explosion mechanism is still plagued by uncertainties which have an impact on the precision with which one can predict time, energy and flavor-dependent neutrino fluxes. On the other hand, the intrinsic neutrino properties are not fully known, since the type of mass hierarchy and the value of the θ_{13} angle are unknown.

The total event rates and the energy spectra of the detected supernova neutrinos depend on the neutrino flavor and on the θ_{13} mixing angle and the type of mass hierarchy. However, it is not a priori easy to separate neutrino and supernova physics. Different solutions to this problem have been proposed. Global fits of data ([7, 8]) and analyses considering qualitative features of the supernova neutrino fluxes ([9]) have been performed for the case of Čerenkov detectors. The potential of liquid scintillator detectors has also been investigated ([10]).

We have already qualitatively illustrated in our paper [11] that four independent channels are a priori accessible with a liquid argon TPC: elastic scattering on electrons, ν_e charged current absorption on argon, $\bar{\nu}_e$ charged current absorption on argon and neutral current interactions on argon. They have different sensitivities to electron-neutrino, anti-electron-neutrino and other neutrino flavors (muon and tau (anti)neutrinos). These events being sensitive to different combinations of neutrino and antineutrino flavors can be combined to over-constrain the features of the supernova fluxes that are at the moment not well constrained by theory and the mixing parameters and allow neutrino and supernova physics effects to be

disentangled.

In the present paper we study quantitatively the capability of LAr TPC detectors to simultaneously measure the supernova and oscillation parameters, performing a global fit to the event energy distribution for elastic and charged current events and to the rate for the neutral current events.

This study is motivated by the 3 kton LAr ICARUS experiment [12] that was proposed at the Gran Sasso laboratory, and by ideas for a very large liquid argon TPC with a mass in the range of 100 ktons (see [13] and independently [14]).

2 Theoretical framework

We briefly summarize in this section the neutrino features relevant for this analysis. We essentially follow the general framework already described in our previous paper [11].

2.1 Supernova physics

At the end of the life of a massive star with a core mass greater than the Chandrasekhar mass, the energy generation in the core stops, and the star undergoes a fast gravitational collapse. Within a duration of tens of milliseconds, this collapse compresses the inner core beyond nuclear matter densities. During this stage electron neutrinos are produced via neutronisation processes. While the electron neutrinos produced could escape the star during the first period (producing the “neutrino burst”), the very dense core becomes opaque to neutrinos which remain captured within the supernova core producing the so-called inner core rebound. This generates a shock wave which propagates radially outward through the star remnants, supplying the “explosion” mechanism. During the shock phase, thermal neutrinos and antineutrinos of all flavors are produced due to high temperatures. It is believed that the 99% of the total binding energy of the star, $E_B \approx 3 \times 10^{53}$ ergs, is emitted in the form of neutrinos. These neutrinos are in equilibrium with their surrounding matter density and their energy spectra can be described by a function close to a Fermi-Dirac distribution. The flux of a neutrino ν_α emitted can then be written as [9]:

$$\phi_\alpha(E_\alpha, L_\alpha, D, T_\alpha, \eta_\alpha) = \frac{L_\alpha}{4\pi D^2 F_3(\eta_\alpha) T_\alpha^4} \frac{E_\alpha^2}{e^{E_\alpha/T_\alpha - \eta_\alpha} + 1} \quad (1)$$

where L_α is the luminosity of the flavor ν_α ($E_B = \sum L_\alpha$), D is the distance to the supernova, E_α is the energy of the ν_α neutrino, T_α is the neutrino temperature inside the neutrinosphere and η_α is the “pinching” factor. We have taken $\eta_\alpha = 0$ and hence no deviations in the high energy tail are considered. The neutrino average energy $\langle E_{\nu_\alpha} \rangle$ depends on both T_α and η_α . For $\eta_\alpha = 0$, $\langle E_{\nu_\alpha} \rangle \approx 3.15 T_\alpha$. The normalization factor in absence of pinching is equal to $F_3(0) \approx 5.68$.

The original ν_μ , ν_τ , $\bar{\nu}_\mu$ and $\bar{\nu}_\tau$ fluxes are approximately equal and therefore we treat them as ν_x . Out of all neutrinos, muon and tau neutrinos and their antiparticles interact with matter through neutral currents only, whereas electron neutrinos and their antiparticles feel both charged and neutral currents. Therefore, muon and tau flavors should decouple first and hence have the largest temperatures. This energy hierarchy between the different neutrino

flavors is generally believed to hold and imply $\langle E_{\nu_e} \rangle < \langle E_{\bar{\nu}_e} \rangle < \langle E_{\nu_x} \rangle$, due to the different strength of neutrino interactions with the surrounding matter. However, the specific neutrino spectra remain a matter of detailed calculations. In particular, the simulations of Raffelt et al. [15] seem to indicate that the energy differences between flavors could be very small. We use a range of typical values of the neutrino average energies and relative luminosities provided by several simulations in the following intervals [9, 15]:

$$\langle E_{\nu_e} \rangle = (7-18) \text{ MeV}; \quad \langle E_{\bar{\nu}_e} \rangle = (14-22) \text{ MeV}; \quad \langle E_{\nu_x} \rangle = (15-35) \text{ MeV} \quad (2)$$

$$L_e/L_x = (0.5-2); \quad L_e = L_{\bar{e}} \quad (3)$$

In practice, we will consider two specific scenarios (I & II) in order to understand the effects of a hierarchical versus non-hierarchical distribution of energies on our results, see below, and take luminosity equipartition. Some detailed simulations may also give rise to cases where the electron luminosities of the neutrinos vary between (0.5–2) times the muon and tau luminosities. We did not explicitly consider this case, even though our calculations could be extended to such a case. We will be later concerned on how well one can determine the energies and the relative luminosities of the neutrinos through the detection of a single supernova collapse.

We consider core collapse supernovae at a distance D of 10 kpc (galactic supernovae). We assume that in the actual event of a supernova, this distance will be precisely estimated by independent astronomical observations and we hence take this value as precisely known in our discussion¹.

In order to parameterize the supernova physics, we employ *five* supernova parameters:

1. the total binding energy $E_B = \sum L_\alpha$,
2. the average energies of the neutrinos emitted from the supernova $\langle E_{\nu_e} \rangle, \langle E_{\bar{\nu}_e} \rangle, \langle E_{\nu_x} \rangle$ and
3. the relative luminosities of the electron and non-electron neutrinos L_e/L_x .

We always assume $L_e = L_{\bar{e}}$ and $L_x = L_{\bar{x}}$, hence we obtain:

$$\begin{aligned} E_B &= L_e + L_{\bar{e}} + 2L_x + 2L_{\bar{x}} = 2L_e + 4L_x \\ &= 2L_x(L_e/L_x + 2) \end{aligned} \quad (4)$$

from which $L_x = L_{\bar{x}} = E_B/(2(L_e/L_x + 2))$.

In order to take into account the uncertainties on the knowledge of the supernova physics, we consider two different sets of reference values for the supernova parameters from Ref. [16] and [15], corresponding to one hierarchical energy scenario (I) and a non-hierarchical energy scenario (II). They differ in the assumptions on the average energies of the neutrino flavors (Table 1).

¹We note that the error on the distance will essentially affect the overall normalization of the fluxes, parameterized by the binding energy in our discussion. This error will not fundamentally affect our conclusions. On the other hand, the fact that a supernova could actually occur at a closer or larger distance does affect the statistics of collected event. We take 10 kpc as a reference value for easy comparison with other authors.

SN scenario	E_B ($\times 10^{53}$ erg)	$\langle E_{\nu_e} \rangle$ (MeV)	$\langle E_{\bar{\nu}_e} \rangle$ (MeV)	$\langle E_{\nu_{\mu,\tau}} \rangle = \langle E_{\bar{\nu}_{\mu,\tau}} \rangle$ (MeV)	Luminosity	Ref.
I	3	11	16	25	$L_{\nu_e} = L_{\bar{\nu}_e} = L_{\nu_x}$	[16]
II	3	13	16	17.6	$L_{\nu_e} = L_{\bar{\nu}_e} = L_{\nu_x}$	[15]

Table 1: Assumed supernova parameters: scenarios I and II.

2.2 Neutrino flavor oscillation physics

We summarize here the supernova flux changes introduced by flavor oscillations (see e.g. Ref. [11] for more details). Before arriving at Earth the neutrino fluxes travel through the supernova mantle undergoing two MSW [6] resonances: one at high density $\rho \approx 10^3\text{--}10^4$ g cm $^{-3}$ (H-resonance) which is governed by the atmospheric parameters (Δm_{31}^2 and θ_{13}) and the other one at low density $\rho \approx 10\text{--}30$ g cm $^{-3}$ (L-resonance), characterized by the solar parameters (Δm_{21}^2 and θ_{12}). The exact propagation of the neutrinos and their oscillation from one flavor to another depend on the matter density profile. We refer the reader to Ref. [11] for more details on our implementation of these effects.

The transitions in the two resonance layers can be considered independently and each transition is reduced to a two neutrino oscillation problem. The H-resonance lies in the neutrino channel for normal mass hierarchy and in the antineutrino channel for the inverted hierarchy. The L-resonance lies in the neutrino channel for both the hierarchies [17].

The propagation through the resonance L is always adiabatic for the LMA solar parameters. In the case of the H resonance, the “jump” probability depends on the θ_{13} angle as [17]:

$$P_H \propto \exp \left[-const \sin^2 \theta_{13} \left(\frac{\Delta m_{31}^2}{E} \right)^{2/3} \right] \quad (5)$$

Considering $P_{ee} = P(\nu_e \rightarrow \nu_e)$ and $\bar{P}_{ee} = P(\bar{\nu}_e \rightarrow \bar{\nu}_e)$ the survival probabilities, the neutrino fluxes arriving at Earth (ϕ_ν) can be written in terms of the fluxes in absence of oscillations (ϕ_ν^o) as:

$$\begin{aligned} \phi_{\nu_e} &= \phi_{\nu_e}^o P_{ee} + \phi_{\nu_x}^o (1 - P_{ee}) \\ \phi_{\bar{\nu}_e} &= \phi_{\bar{\nu}_e}^o \bar{P}_{ee} + \phi_{\bar{\nu}_x}^o (1 - \bar{P}_{ee}) \\ \phi_{\nu_\mu} + \phi_{\nu_\tau} &= \phi_{\nu_e}^o (1 - P_{ee}) + \phi_{\nu_x}^o (1 + P_{ee}) \\ \phi_{\bar{\nu}_\mu} + \phi_{\bar{\nu}_\tau} &= \phi_{\bar{\nu}_e}^o (1 - \bar{P}_{ee}) + \phi_{\bar{\nu}_x}^o (1 + \bar{P}_{ee}) \end{aligned} \quad (6)$$

with $\phi_{\nu_x}^o = \phi_{\nu_\mu}^o = \phi_{\nu_\tau}^o = \phi_{\bar{\nu}_x}^o = \phi_{\bar{\nu}_\mu}^o = \phi_{\bar{\nu}_\tau}^o$.

Using a standard parametrization of the mixing matrix and considering that the neutrino bursts do not cross the Earth, the survival probabilities can be expressed in terms of the “jump” probability in the H resonance P_H :

$$\begin{aligned} P_{ee} &= P_H \sin^2 \theta_{12} \cos^2 \theta_{13} + (1 - P_H) \sin^2 \theta_{13} \\ \bar{P}_{ee} &= \cos^2 \theta_{12} \cos^2 \theta_{13} \end{aligned} \quad (7)$$

for normal hierarchy ($\Delta m_{32}^2 > 0$) and

$$\begin{aligned} P_{ee} &= \sin^2 \theta_{12} \cos^2 \theta_{13} \\ \bar{P}_{ee} &= P_H \cos^2 \theta_{12} \cos^2 \theta_{13} + (1 - P_H) \sin^2 \theta_{13} \end{aligned} \quad (8)$$

for inverted hierarchy ($\Delta m_{32}^2 < 0$).

The following neutrino oscillations parameters have been used, obtained from other neutrino observations [4, 5]:

$$\begin{aligned} \sin^2 2\theta_{23} &= 1. & |\Delta m_{32}^2| &\approx |\Delta m_{31}^2| = 3 \times 10^{-3} eV^2 \\ \sin^2 \theta_{12} &= 0.3 & \Delta m_{21}^2 &= 7 \times 10^{-5} eV^2 \\ \sin^2 \theta_{13} &< 0.02 \text{ (at 90\% C.L.)} & \Delta m_{31}^2 &> 0 \text{ or } \Delta m_{31}^2 < 0 \end{aligned} \quad (9)$$

According to the adiabaticity conditions on the H resonance and the value of the θ_{13} angle, we can consider two limits: the *small mixing angle (S)* ($\sin^2 \theta_{13} < 2 \times 10^{-6}$) and the *large mixing angle (L)* case ($\sin^2 \theta_{13} > 3 \times 10^{-4}$). The value of the survival probabilities and the neutrino fluxes at Earth in these regions are summarized in Table 2 for both mass hierarchies. For intermediate mixing angle values ($2 \times 10^{-6} < \sin^2 \theta_{13} < 3 \times 10^{-4}$), the “jump” probability P_H depends on θ_{13} and on the neutrino energy (see e.g. Ref. [11]).

We can distinguish four extreme cases depending only on the type of mass hierarchy and the value of the θ_{13} mixing angle:

1. **n.h.-L** for normal mass hierarchy and large θ_{13} ,
2. **n.h.-S** for normal hierarchy and small θ_{13} ,
3. **i.h.-L** for inverted mass hierarchy and large θ_{13} ,
4. **i.h.-S** for inverted mass hierarchy and small θ_{13} .

For instance, we select the mixing angle $\sin^2 \theta_{13} = 10^{-3}$ for the large θ_{13} case and $\sin^2 \theta_{13} = 10^{-7}$ for the small θ_{13} case.

These results have been discussed in Ref. [11]. We recall here the salient feature that for normal hierarchy and large mixing angle, the ν_e flux on Earth is fully dominated by ν_x neutrinos in the core of the supernova due to the phenomenon of adiabatic conversion. Similarly, for antineutrinos for inverted hierarchy and large mixing angle.

Limit oscillation scenarios	Survival probabilities $P_{ee} = P(\nu_e \rightarrow \nu_e)$	Neutrino fluxes at Earth $\phi_\alpha^o = \text{w/o osc}, \phi_\alpha = \text{with osc}$
n.h.-L $\sin^2 \theta_{13} > 3 \times 10^{-4}$	$P_{ee} = 0.$ $\overline{P}_{ee} = 0.7$	$\phi_{\nu_e} = \phi_{\nu_x}^o$ $\phi_{\bar{\nu}_e} = 0.7 \phi_{\bar{\nu}_e}^o + 0.3 \phi_{\bar{\nu}_x}^o$ $\phi_{\nu_\mu + \nu_\tau + \bar{\nu}_\mu + \bar{\nu}_\tau} = \phi_{\nu_e}^o + 0.3 \phi_{\bar{\nu}_e}^o + 2.7 \phi_{\nu_x}^o$
n.h.-S or i.h.-S $\sin^2 \theta_{13} < 2 \times 10^{-6}$	$P_{ee} = 0.3$ $\overline{P}_{ee} = 0.7$	$\phi_{\nu_e} = 0.3 \phi_{\nu_e}^o + 0.7 \phi_{\nu_x}^o$ $\phi_{\bar{\nu}_e} = 0.7 \phi_{\bar{\nu}_e}^o + 0.3 \phi_{\bar{\nu}_x}^o$ $\phi_{\nu_\mu + \nu_\tau + \bar{\nu}_\mu + \bar{\nu}_\tau} = 0.7 \phi_{\nu_e}^o + 0.3 \phi_{\bar{\nu}_e}^o + 3 \phi_{\nu_x}^o$
i.h.-L $\sin^2 \theta_{13} > 3 \times 10^{-4}$	$P_{ee} = 0.3$ $\overline{P}_{ee} = 0.$	$\phi_{\nu_e} = 0.3 \phi_{\nu_e}^o + 0.7 \phi_{\nu_x}^o$ $\phi_{\bar{\nu}_e} = \phi_{\nu_x}^o$ $\phi_{\nu_\mu + \nu_\tau + \bar{\nu}_\mu + \bar{\nu}_\tau} = 0.7 \phi_{\nu_e}^o + \phi_{\bar{\nu}_e}^o + 2.3 \phi_{\nu_x}^o$

Table 2: Survival probabilities for ν_e and $\bar{\nu}_e$ and neutrino fluxes at Earth (ϕ_ν) for normal and inverted mass hierarchies and large (L) or small (S) mixing angle θ_{13} in terms of the fluxes (ϕ_ν^o) in absence of oscillations.

3 Supernova neutrino signal in LAr

In a liquid argon TPC supernova neutrinos ($E_\nu < 100$ MeV) can be detected through four different channels ([11]):

1. charged-current (CC) interactions on argon

$$\nu_e {}^{40}\text{Ar} \rightarrow e^- + A' + nN \quad (10)$$

$$\bar{\nu}_e {}^{40}\text{Ar} \rightarrow e^+ + A' + nN \quad (11)$$

where A' is the remnant nucleus and nN represent emitted nucleons or other debris (α 's, ...) (if any). At low energy (< 30 MeV) or at low Q^2 , the dominant reactions are $\nu_e {}^{40}\text{Ar} \rightarrow e^- {}^{40}\text{K}^*$ and $\bar{\nu}_e {}^{40}\text{Ar} \rightarrow e^+ {}^{40}\text{Cl}^*$. The neutrino energy thresholds of these reactions are 1.5 MeV and 7.48 MeV, respectively. The associated photons emitted in the de-excitation of the final state nucleus can be used to separate the two reactions.

2. neutral-current (NC) interactions on argon

$$(\bar{\nu}) {}^{40}\text{Ar} \rightarrow (\bar{\nu}) + A' + nN \quad (12)$$

where A' is the remnant nucleus and nN represent emitted nucleons or other debris (α 's, ...) (if any). At low energy (< 30 MeV) or at low Q^2 , the dominant reaction is $(\bar{\nu}) {}^{40}\text{Ar} \rightarrow (\bar{\nu}) {}^{40}\text{Ar}^*$. The energy threshold of this reaction is 1.46 MeV. The associated photons emitted in the de-excitation of the final state nucleus can be used to identify the reaction.

3. elastic scattering (ELAS) on electrons

$$(\bar{\nu}) e^- \rightarrow (\bar{\nu}) e^- \quad (13)$$

All these channels have been described in more details in reference [11]. We use the nuclear cross sections of the CC and NC processes on argon that have been calculated by Random Phase Approximation (RPA) for neutrino energies up to 100 MeV including all the possible multipoles ([18]). These processes are very important on argon because their high cross sections. As already mentioned, it is possible to separate the different channels by measuring the associated photons from the K , Cl or Ar de-excitation, or by the absence of them in the case of elastic scattering. We recall here that the energy dependence of the cross-section is $\propto E^2$ for the nuclear processes and $\propto E$ for the scattering off electrons.

Table 3 shows the expected number of neutrino events from a supernova at 10 kpc in a 100 kton detector. The four detection channels are considered independently and oscillation and non-oscillation cases are computed for normal and inverted hierarchies. The supernova parameters correspond to scenario I. No threshold on the electron energy has been applied since the burst nature of the supernova signal allows to set trigger and detection thresholds at the level of the MeV.

Scenario I: expected events in 100 kton detector $\langle E_{\nu_e} \rangle = 11 \text{ MeV}, \langle E_{\bar{\nu}_e} \rangle = 16 \text{ MeV}, \langle E_{\nu_x} \rangle = \langle E_{\bar{\nu}_x} \rangle = 25 \text{ MeV}$ and luminosity equipartition					
Reaction	Without oscillation	Oscillation (n.h.)		Oscillation (i.h.)	
		Large θ_{13}	Small θ_{13}	Large θ_{13}	Small θ_{13}
ELAS	1330	1330	1330	1330	1330
$\nu_e \text{CC}$	6240	31320	23820	23820	23820
$\bar{\nu}_e \text{CC}$	540	1110	1110	2420	1110
NC	30440	30440	30440	30440	30440
TOTAL	38550	64200	56700	58010	56700

Table 3: Expected neutrino events in a 100 kton detector from a supernova at a distance of 10 kpc.

3.1 Charged current events

In order to understand the dependencies of the expected number of events with the supernova parameters and the θ_{13} mixing angle, we perform a scan of these parameters for the $\nu_e \text{CC}$, and $\bar{\nu}_e \text{CC}$ processes on argon. While we scan two parameters, the rest are fixed according to the values of scenario I.

Figure 1 shows the expected number of $\nu_e \text{CC}$ events in a 3 kton detector as a function of $\sin^2 \theta_{13}$ and the $\langle E_{\nu_e} \rangle$ and $\langle E_{\nu_x} \rangle$ average energies for a normal mass hierarchy. The range of the parameters is determined by possible physical regions discussed in Section 2.1, namely $\langle E_{\nu_e} \rangle = (7-18) \text{ MeV}$ and $\langle E_{\nu_x} \rangle = (15-35) \text{ MeV}$. We can see from these figures that large and small mixing angle cases are not symmetric and the results depend on the value of the neutrino average energy. $\nu_e \text{CC}$ events are very sensitive to the $\langle E_{\nu_e} \rangle$ and $\langle E_{\nu_x} \rangle$ energies while they are of course independent on the $\langle E_{\bar{\nu}_e} \rangle$ value.

For large θ_{13} mixing angle, maximal flavor conversion occurs and all $\nu_{\mu,\tau}$ neutrinos convert into ν_e 's (see Table 2). Therefore, the number of expected events will only depend on the original average energy of ν_x neutrinos and not on $\langle E_{\nu_e} \rangle$, as can be seen in the figures. For small θ_{13} mixing angle the expected flux of ν_e 's at the detector is $\approx 30\%$ of original ν_e and $\approx 70\%$ of ν_x neutrinos produced in the supernova. In this case, the number of $\nu_e \text{CC}$ increases linearly with $\langle E_{\nu_e} \rangle$ and $\langle E_{\nu_x} \rangle$.

Figure 2 shows the number of $\bar{\nu}_e \text{CC}$ events expected in a 3 kton detector as a function of $\sin^2 \theta_{13}$ and the $\langle E_{\bar{\nu}_e} \rangle$ and $\langle E_{\nu_x} \rangle$ energies for the case of inverted hierarchy. The H resonance lies in the antineutrino channel for the inverted hierarchy and therefore the behavior of the $\bar{\nu}_e \text{CC}$ rates for i.h. is quite similar to the $\nu_e \text{CC}$ for n.h. In the first case the variations between small and large mixing angle are more pronounced than for $\nu_e \text{CC}$ but the event rates statistics are smaller.

The two channels $\nu_e \text{CC}$ and $\bar{\nu}_e \text{CC}$ are sensitive to the θ_{13} mixing angle and to the mass hierarchy but in different ways. This will help to distinguish the oscillation scenarios.

3.2 Neutral current events

Similarly, we perform a scan of the parameters for the NC processes on argon. While we scan two parameters, the rest are fixed according to the values of scenario I.

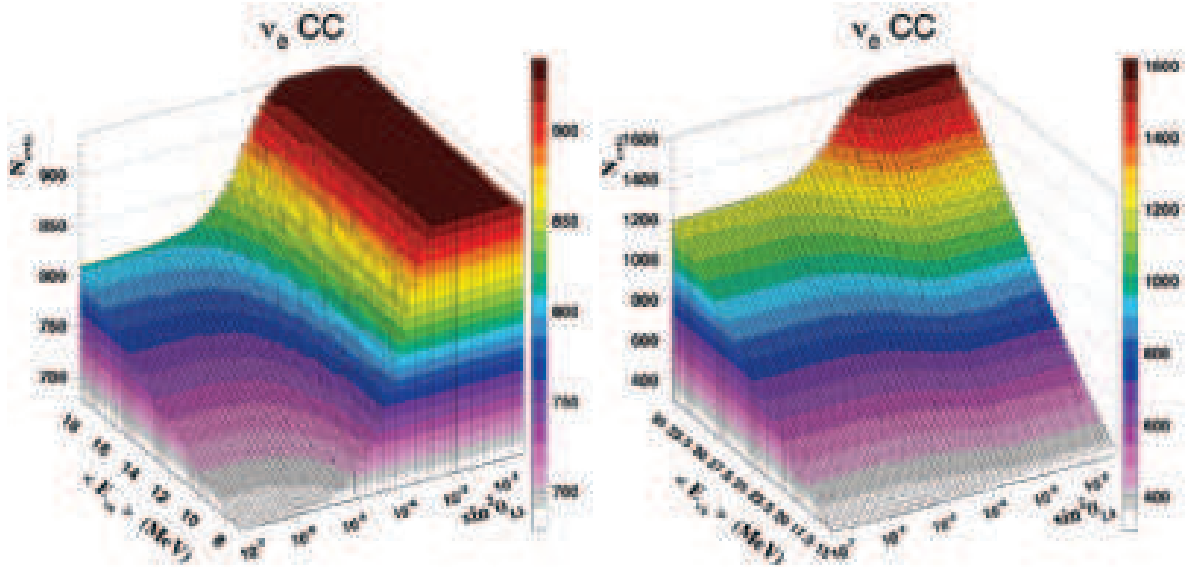


Figure 1: **Normal mass hierarchy:** Variation of the expected number of ν_e CC events in a 3 kton detector as a function of $\sin^2 \theta_{13}$ and the original supernova neutrino average energies $\langle E_{\nu_e} \rangle$ and $\langle E_{\nu_x} \rangle$.

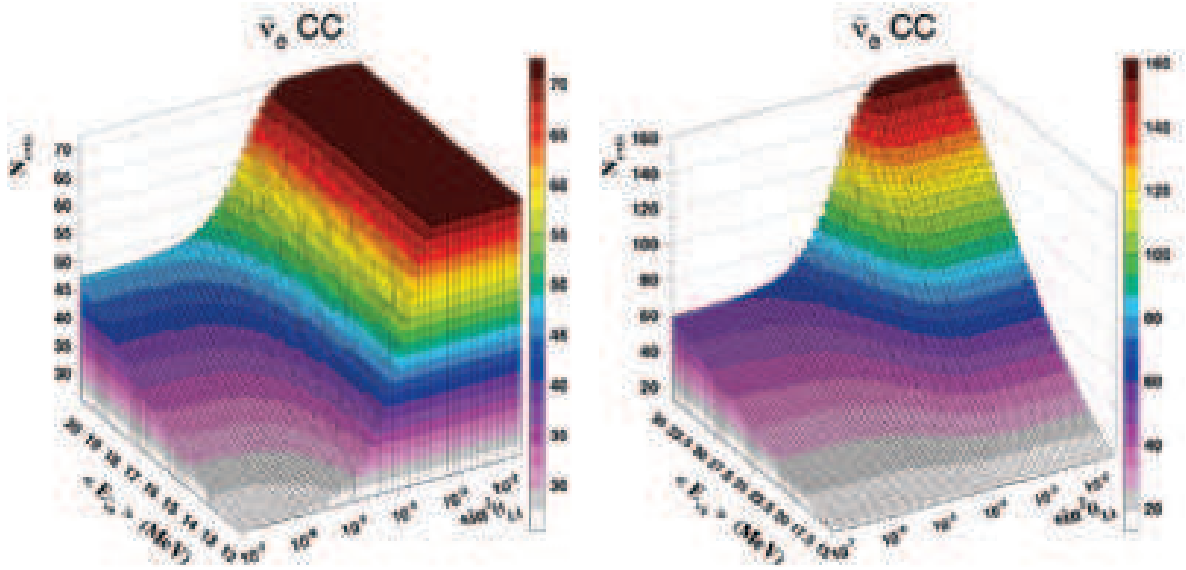


Figure 2: **Inverted mass hierarchy:** Variation of the expected number of $\bar{\nu}_e$ CC events in a 3 kton detector as a function of $\sin^2 \theta_{13}$ and the original supernova neutrino average energies $\langle E_{\bar{\nu}_e} \rangle$ and $\langle E_{\nu_x} \rangle$.

Figure 3 shows the variation of the expected events from the NC process with several supernova parameters normalized to a 3 kton detector.

In the first plot we see the dependence of the NC events with the original average energies $\langle E_{\nu_e} \rangle$ and $\langle E_{\nu_x} \rangle$ within the ranges defined in Section 2.1, namely $\langle E_{\nu_e} \rangle = (7-18)$ MeV and $\langle E_{\nu_x} \rangle = (15-35)$ MeV. Since neutral currents are by definition flavor independent, they are not sensitive to the θ_{13} mixing angle. The number of events increases quickly with average energies because of the quadratic dependence of the NC cross section on argon. The variations within the range of considered energies of ν_x are large while within the range of the $\langle E_{\nu_e} \rangle$, the variation is much smaller.

In the second and third plots we scan the average energies as a function of the ratio between the electron and non-electron neutrino luminosities (L_e/L_x). As L_e/L_x increases, the flux of ν_e 's is increasing with respect to the ν_x 's. Accordingly, the number of NC events decreases because ν_e 's are assumed to be less energetic than ν_x 's. We can see that the number of events increases with $\langle E_{\nu_x} \rangle$ and $\langle E_{\nu_e} \rangle$.

The last plot shows the variations with $\langle E_{\nu_x} \rangle$ and the total binding energy E_B . For low $\langle E_{\nu_x} \rangle$ energy, the number of events is almost constant. But as soon as the ν_x energy increases, the changes with E_B are much bigger, given the quadratic dependence of the cross-section on energy.

All these figures show that the NC events are very sensitive to the different supernova parameters independently of the neutrino oscillations. This process hence constitutes an excellent probe for the supernova properties independent of the neutrino oscillation physics. The combination of the information extracted from other interactions on argon with NC will allow to decouple supernova from oscillation physics.

Elastic events off electrons are also in part sensitive to all neutrino and antineutrino flavors. We note however that the rate of NC events is much larger than that of elastic events (see Table 3), hence, the statistical power of the nuclear NC events is much larger than that of elastic events on electrons.

3.3 Energy distribution of the charged current and elastic events

We have presented how the expected rates of the different processes change depending on θ_{13} , the mass hierarchy and the astrophysical parameters. But also the energy spectra of the neutrinos is affected by the value of these parameters. See our reference [11] for examples of the variations of the spectra for different values of the θ_{13} parameter and mass hierarchies.

Figures 4 and 5 show the variation of the neutrino energy spectra for the elastic scattering, ν_e CC and $\bar{\nu}_e$ CC processes as a function of the $\langle E_{\nu_x} \rangle$ average energy in the case of large mixing angle ($\sin^2 \theta_{13} = 10^{-3}$) and normal or inverted mass hierarchies, respectively. The total number of events corresponds to the expectations for a 3 kton detector. We have taken energy bins of 1 MeV.

As we consider a large θ_{13} mixing angle, the ν_e flux arriving at Earth is $\phi_{\nu_e} \simeq \phi_{\nu_x}^o (\langle E_{\nu_x} \rangle)$. The energy distribution of the ν_e CC events depends strongly on the $\langle E_{\nu_x} \rangle$ parameter. For the inverted mass hierarchy, the main variations as a function of $\langle E_{\nu_x} \rangle$ are for the $\bar{\nu}_e$ CC events.

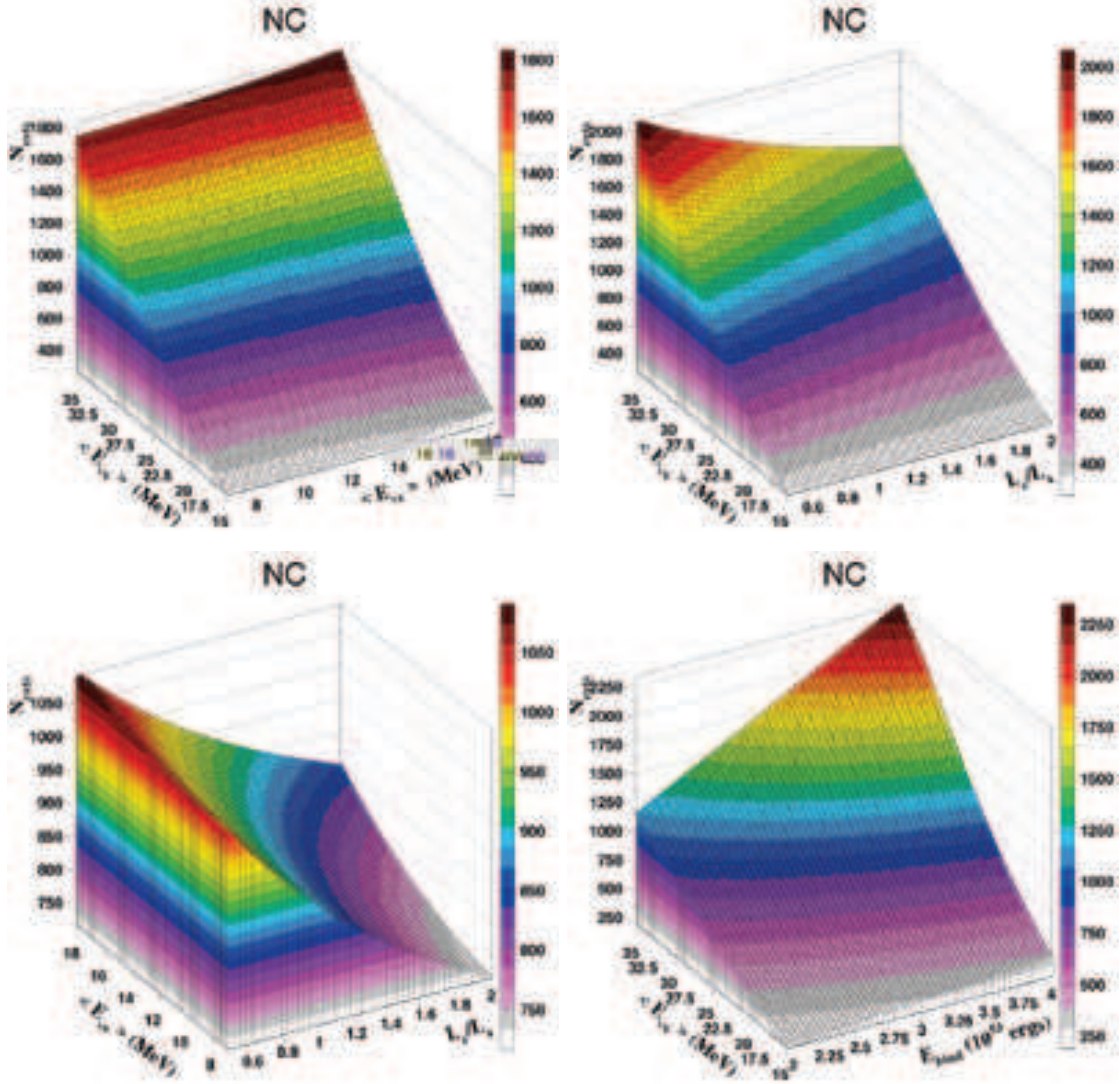


Figure 3: Variation of the expected number of NC events in a 3 kton detector as a function of the original supernova ν_e and ν_x average energies, the ratio between the electron and non-electron neutrino luminosities (L_e/L_x) and the total binding energy (E_B).

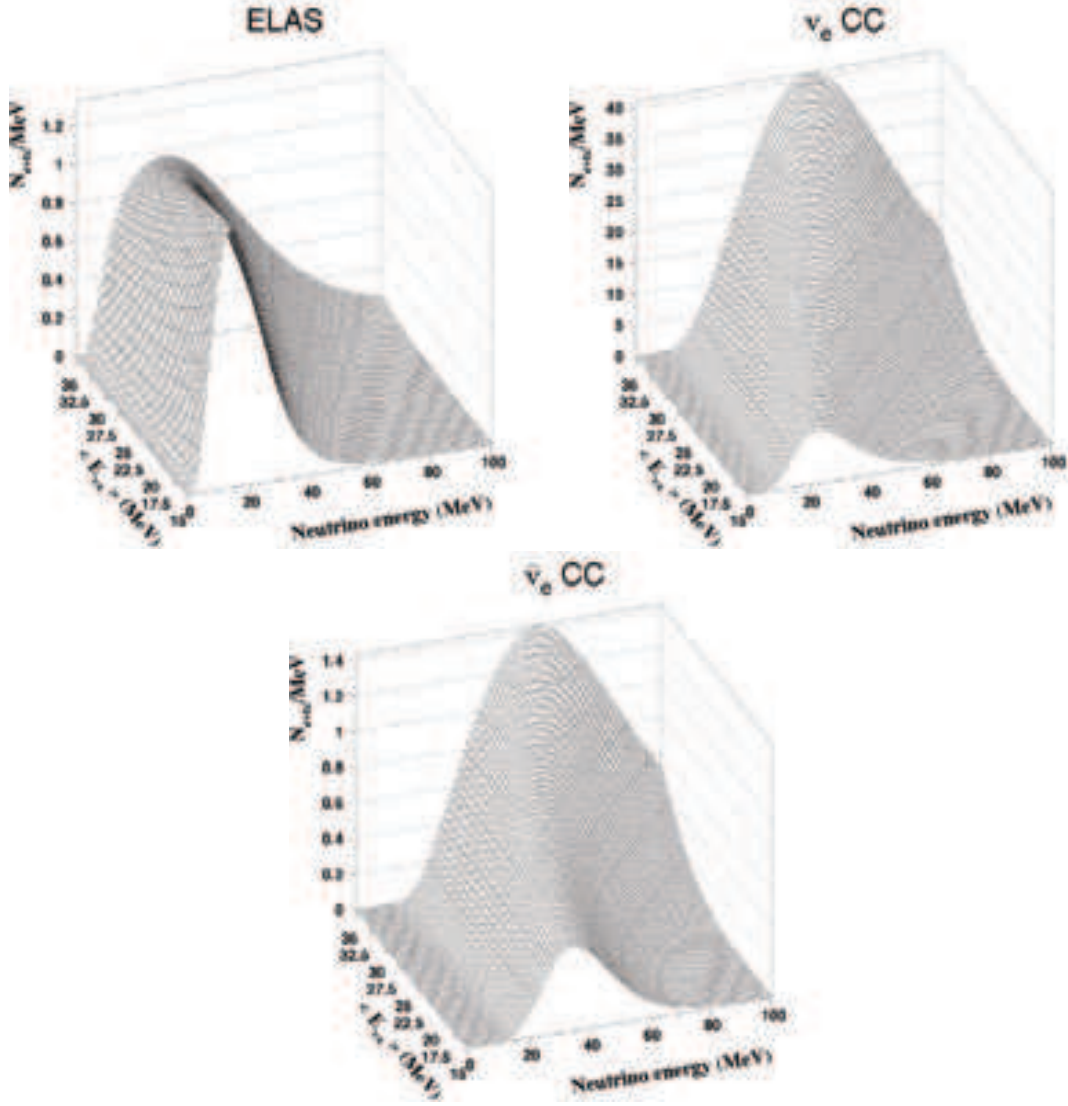


Figure 4: **Large mixing angle** ($\sin^2 \theta_{13} = 10^{-3}$) **and normal mass hierarchy**: Neutrino energy spectra for the elastic scattering, ν_e CC and $\bar{\nu}_e$ CC interaction processes on argon as a function of the $\langle E_{\nu_x} \rangle$ average energy. The distributions are normalized to a 3 kton detector.

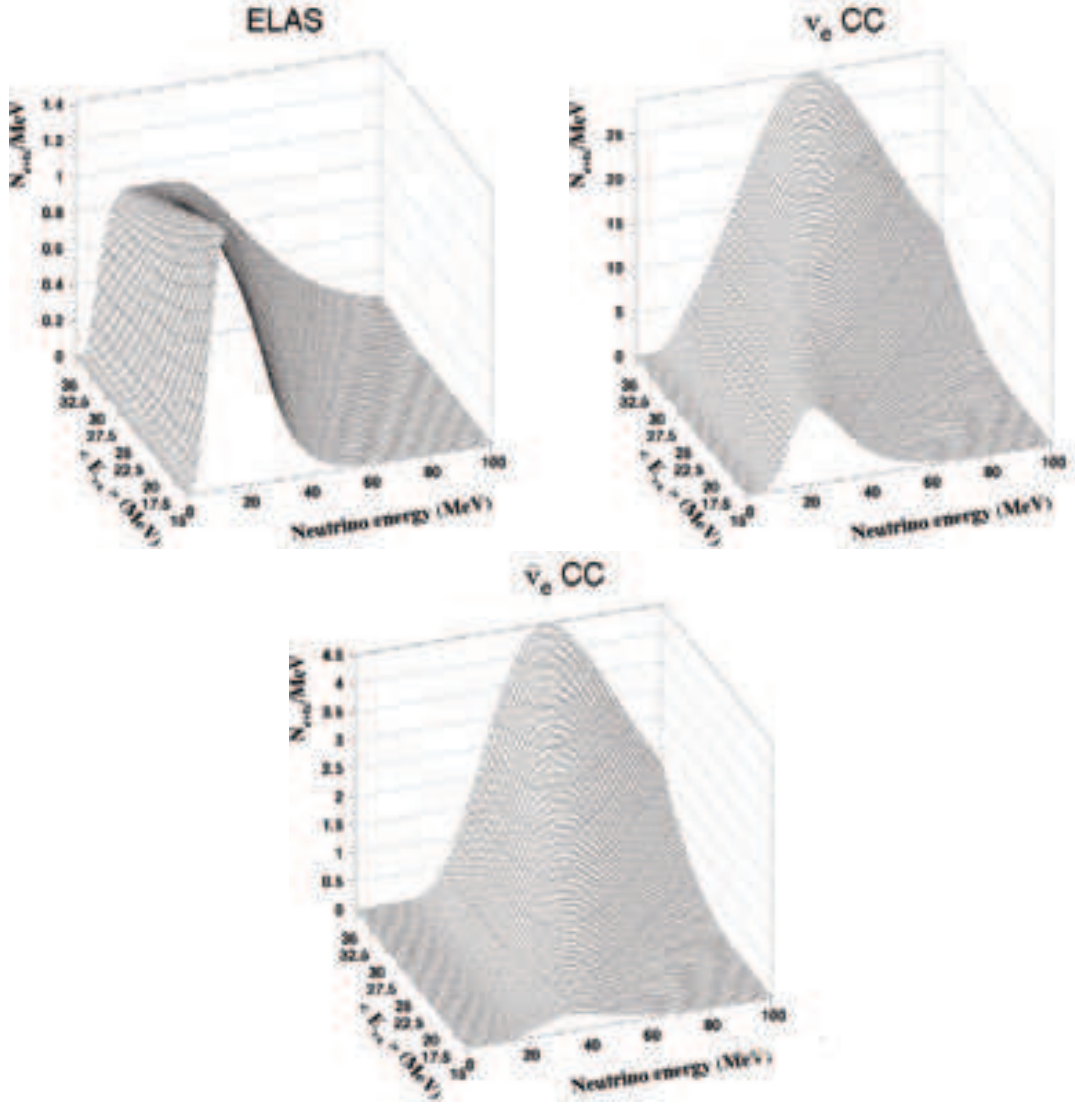


Figure 5: **Large mixing angle** ($\sin^2 \theta_{13} = 10^{-3}$) **and inverted mass hierarchy**: Neutrino energy spectra for the elastic scattering, ν_e CC and $\bar{\nu}_e$ CC interaction processes on argon as a function of the $\langle E_{\nu_x} \rangle$ average energy. The distributions are normalized to a 3 kton detector.

4 Analysis procedure

We will consider three different situations. In all cases, we exploit the information from the four neutrino detection channels (ELAS, ν_e CC, $\bar{\nu}_e$ CC and NC). When relevant, we compare the results with the case of not having access to NC events, which is experimentally the most challenging signature.

1. **Study of the different oscillation scenarios without knowledge of the supernova parameters:** We investigate the sensitivity to the θ_{13} and mass hierarchy parameters without any assumption on the supernova parameters. Quantitative results on the determination of the $\sin^2 \theta_{13}$ mixing angle are obtained. This is described in Section 5.
2. **Study of the supernova parameters assuming that the oscillation parameters are known:** Assuming that we know the value of the oscillation parameters from terrestrial experiments, we study the possible determination of the *five* supernova parameters E_B , $\langle E_{\nu_e} \rangle$, $\langle E_{\bar{\nu}_e} \rangle$, $\langle E_{\nu_x} \rangle$ and L_e/L_x . Two cases are assumed: (a) the θ_{13} is large ($\sin^2 \theta_{13} = 10^{-3}$) and has been measured with a 10% precision from long-baseline experiments; (b) the θ_{13} is small ($\sin^2 \theta_{13} < 10^{-4}$) and an upper limit on its value has been determined. This is described in Section 6.
3. **Study of the supernova parameters without any knowledge on the neutrino oscillation parameters:** We investigate the information that can be extracted from supernova neutrinos if a supernova explosion occurred nowadays when no information about the oscillation parameters θ_{13} and mass hierarchy ($\text{sign}[\Delta m_{32}^2]$) is available. This is described in Section 7.

As was shown in the previous section, the simultaneous observation of ELAS, ν_e CC, $\bar{\nu}_e$ CC and NC events on argon enables us to extract information about the oscillation parameters θ_{13} and the type of mass hierarchy ($\text{sign}[\Delta m_{32}^2]$) and the five supernova parameters.

In order to determine all these parameters quantitatively we use a χ^2 method. This analysis procedure includes all the uncertainties and parameter correlations. We define a set of reference values for the relevant supernova and oscillation parameters that we consider as “true”. Different values of the θ_{13} angle are chosen in the analysis for normal and inverted mass hierarchies. Two sets of reference values of the astrophysical parameters are studied according to scenarios I and II described in Table 1.

To see how well we can discriminate every “true” scenario, we minimize the χ^2 in the space of the five astrophysical parameters and the two oscillation parameters. The χ^2 function is defined as:

$$\chi^2(x) = \sum_{i=1}^{N_{bins}} \frac{(N_i(x) - N_i(x^0))^2}{\sigma_i^2(x)} \quad (14)$$

where N_{bins} is the number of bins considered in every histogram; N_i is the number of events per bin i ; σ is the statistical error associated to the bin i ; x corresponds to the set of parameters to be determined $x \equiv \{E_B, \langle E_{\nu_e} \rangle, \langle E_{\bar{\nu}_e} \rangle, \langle E_{\nu_x} \rangle, L_e/L_x, \sin^2 \theta_{13}, \text{sign}[\Delta m_{32}^2]\}$, which are freely varying and x^0 are the “true” values of these parameters. When computing the χ^2 for one parameter, the others are left free. In this way, we can naturally take into

account the uncertainty on the given parameter introduced by the lack of knowledge on the others. This is particularly relevant in the discussion of the decoupling of supernova and oscillation parameters.

The total χ^2 is computed as the sum of the minimized χ^2 corresponding to every detection channel:

$$\chi_{total}^2 = \chi_{ELAS}^2 + \chi_{\nu_e CC}^2 + \chi_{\bar{\nu}_e CC}^2 + \chi_{NC}^2 \quad (15)$$

The fit is performed with the MINUIT [19] package, and is expected to get back the same values of the parameters, starting from the reference distributions. At each iteration, a different set of parameters is probed, and with the same procedure used to get the reference histograms. The condition of the hierarchy between the average energies, confirmed by various supernova simulations, is enforced during the minimization:

$$\langle E_{\nu_e} \rangle \leq \langle E_{\bar{\nu}_e} \rangle \leq \langle E_{\nu_x} \rangle \quad (16)$$

Otherwise, the ranges of the parameters are left free.

We compare the energy distributions of the elastic scattering, $\nu_e CC$ and $\bar{\nu}_e CC$ neutrino events from the “true” scenarios with those obtained with all possible values of the parameters, taking into account the oscillations inside the SN matter. A bin width of 1 MeV is considered in the spectra. For the NC channel, the energy distribution cannot be determined due to the neutrino presence in the final state. We only consider the number of NC events in the fit.

In order to compute the precision of the determination of the parameters, we consider two methods: (1) a one-dimensional “scan” of a given parameter; the other variables are left free and minimized at each step; the resp. 1, 2, 3 sigmas are given by resp. $\chi_{min}^2 + 1$, $+4$ and $+9$. (2) a two-dimensional “scan” of a two-parameter plane; the other variables are left free and minimized at each point in the plane; the resp. 68%, 90%, 99% C.L. are given by resp. $\chi_{min}^2 + 2.4$, $+4.6$ and $+9.2$.

5 Study of the different oscillation scenarios without knowledge of the supernova parameters

In this first section we investigate the possible oscillation scenarios without any assumption on the supernova properties.

As was shown in table 2, the value of the survival probabilities P_{ee} and \bar{P}_{ee} is constant in two extreme regions of the θ_{13} parameter: the large mixing angle case ($\sin^2 \theta_{13} > 3 \times 10^{-4}$) and the small mixing angle case ($\sin^2 \theta_{13} < 2 \times 10^{-6}$). It means that the neutrino fluxes do not change with θ_{13} in these regions. On the other hand, if the angle is in an intermediate range $2 \times 10^{-6} < \sin^2 \theta_{13} < 3 \times 10^{-4}$, the fluxes depend on the θ_{13} value and on the neutrino energy. Hence, different energy spectra and event rates are expected for every θ_{13} value.

For this reason we first analyze the true small and large mixing angle scenarios and study the possibility to distinguish the mass hierarchy and put a bound on the θ_{13} value. Then, we investigate different values of the angle in the intermediate region and we determine the statistical accuracy with which it can be measured.

5.1 Small and large mixing angle extreme cases

We consider the four extreme oscillation cases (see Section 2.2) as possible “true” values and we use the information of the neutrino detection channels to discriminate between them. Because we assume no knowledge on the original supernova neutrino parameters, we let them free while performing the χ^2 minimization. For example, for every value of the θ_{13} and a fixed hierarchy, we vary the supernova parameters in order to obtain the set of values that minimize the χ^2 function for this given value of the mixing angle and mass hierarchy. The χ^2 value result of this fit can then be studied as a function of θ_{13} and the mass hierarchy.

A summary of the results on the determination on the θ_{13} mixing angle for the different oscillation cases can be found in Table 4. We include the results for a 3 kton and a 100 kton detector and supernova scenarios I and II.

Determination of θ_{13} and mass hierarchy (SN parameters free)					
“True” osc. case	3 kton LAr		100 kton LAr		Events type
	$\sin^2 \theta_{13}$ and assumed hierarchy SN scen I	SN scen II	$\sin^2 \theta_{13}$ and assumed hierarchy SN scen I	SN scen II	
n.h.-L	$> 2.1 \times 10^{-4}$ n.h. excluded i.h.	$> 6.2 \times 10^{-5}$ n.h. excluded i.h.	$> 4.5 \times 10^{-4}$ n.h. excluded i.h.	$> 1.8 \times 10^{-4}$ n.h. excluded i.h.	all all
	$> 7.5 \times 10^{-5}$ n.h. excluded i.h.	– –	$> 2.5 \times 10^{-4}$ n.h. excluded i.h.	$> 9.4 \times 10^{-5}$ n.h. excluded i.h.	no NC no NC
n.h.-S	$< 2.4 \times 10^{-5}$ n.h. $< 3.8 \times 10^{-5}$ i.h.	– –	$< 4.3 \times 10^{-6}$ n.h. $< 5.9 \times 10^{-6}$ i.h.	$< 1.2 \times 10^{-5}$ n.h. $< 4.3 \times 10^{-6}$ i.h.	all all
	$< 3.7 \times 10^{-5}$ n.h. $< 4.1 \times 10^{-5}$ i.h.	– –	$< 7.3 \times 10^{-6}$ n.h. $< 7.3 \times 10^{-6}$ i.h.	$< 3.2 \times 10^{-5}$ n.h. $< 1.1 \times 10^{-4}$ i.h.	no NC no NC
i.h.-L	excluded n.h. $> 2.3 \times 10^{-4}$ i.h.	– –	excluded n.h. $> 5.0 \times 10^{-4}$ i.h.	excluded n.h. $> 2.3 \times 10^{-4}$ i.h.	all all
	$< 2.8 \times 10^{-5}$ n.h. –	– –	excluded n.h. $> 4.9 \times 10^{-4}$ i.h.	$< 2.0 \times 10^{-5}$ n.h. –	no NC no NC
i.h.-S	$< 2.4 \times 10^{-5}$ n.h. $< 3.8 \times 10^{-5}$ i.h.	– –	$< 5.9 \times 10^{-6}$ n.h. $< 4.0 \times 10^{-6}$ i.h.	$< 1.2 \times 10^{-5}$ n.h. $< 4.1 \times 10^{-5}$ i.h.	all all
	$< 3.7 \times 10^{-5}$ n.h. $< 4.6 \times 10^{-5}$ i.h.	– –	$< 7.2 \times 10^{-6}$ n.h. $< 7.4 \times 10^{-6}$ i.h.	$< 3.2 \times 10^{-5}$ n.h. $< 1.1 \times 10^{-4}$ i.h.	no NC no NC

Table 4: Estimated limit on the θ_{13} mixing angle at 1σ for different “true” oscillation cases with a 3 and a 100 kton detectors. We compare the results considering as reference values for the supernova neutrino parameters scenarios I (hierarchical) and II (non-hierarchical).

5.1.1 Supernova scenario I and 3 kton detector

We first discuss results for a 3 kton detector. Plots in figure 6 show the variation of the minimized χ^2 value with the $\sin^2 \theta_{13}$ parameter and the mass hierarchy. In the top right corner of the figure is indicated in bold the “true” scenario considered (the x^0 parameters). The left part of a given plot corresponds to the results of the fit *under the assumption of normal hierarchy and the right part for an inverted hierarchy*.

Solid lines are computed considering the four supernova neutrino detection channels. Dashed lines do not take into account the NC processes, only ELAS and CC events. The one- and two- sigma levels are shown by horizontal lines. The four plots on resp. the top

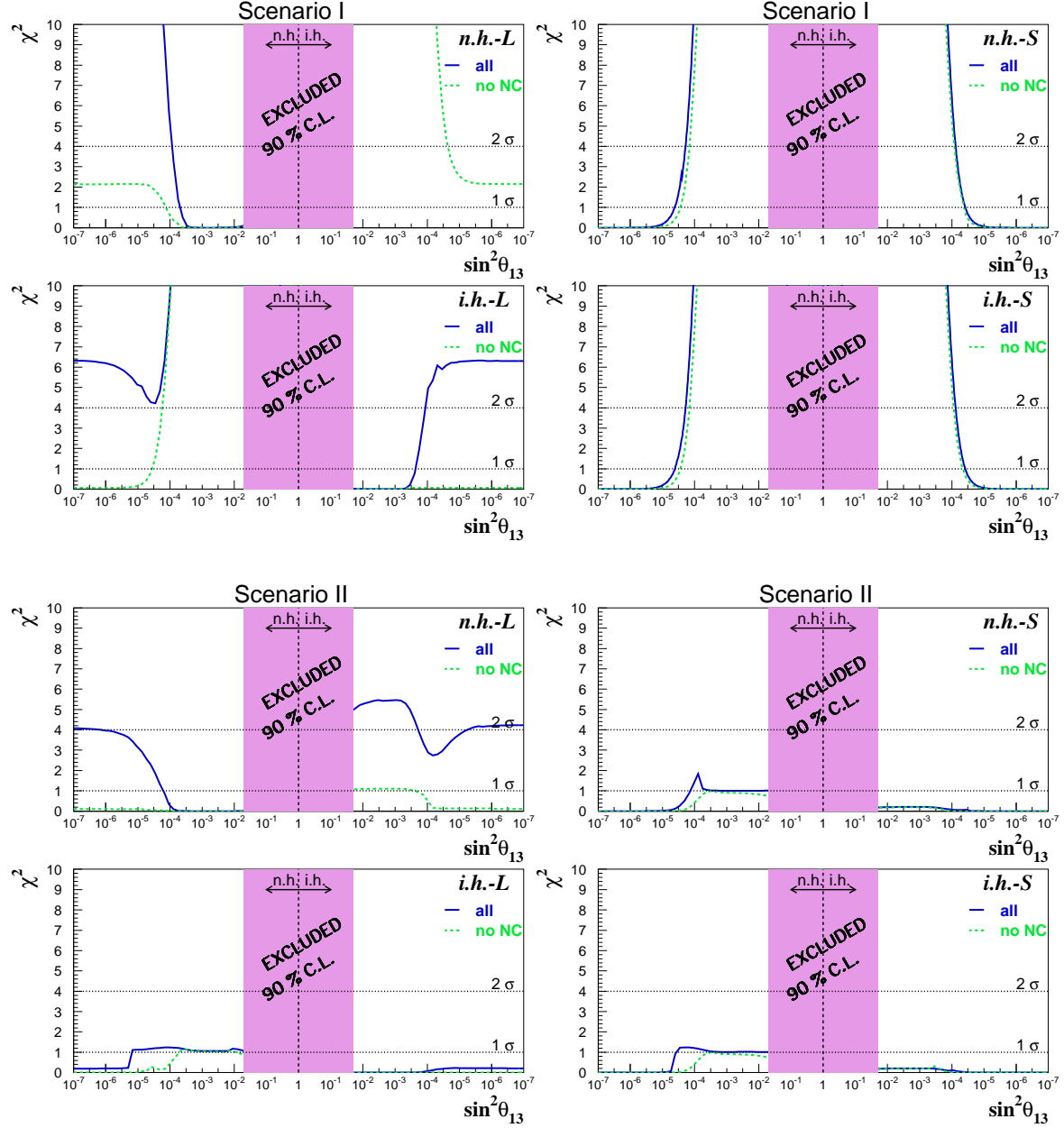


Figure 6: **Extreme mixing angle cases and 3 kton detector:** χ^2 value of the fit as a function of $\sin^2 \theta_{13}$ for a 3 kton detector. Curves on the left (right) part of every plot correspond to the results of the fit under the assumption of normal (inverted) hierarchy. Four limiting oscillation scenarios (n.h.-L, n.h.-S, i.h.-L, i.h.-S) are considered as “true” and the reference values of the supernova parameters correspond to scenario I (top) and II (bottom). Solid curves are computed using the information of the four supernova neutrino detection processes and the dashed line does not take into account NC events.

(bottom) are obtained using as true supernova parameters those from resp. scenario I (II). The shaded region illustrates the excluded region by the results of reactor experiments [5].

We see that normal and inverted hierarchies are indistinguishable for small “true” θ_{13} mixing angle. The results of the fit are similar and only an upper bound on $\sin^2 \theta_{13}$ can be set. This limit is $\sin^2 \theta_{13} < 2.4 \times 10^{-5}$ for assumed n.h. and $\sin^2 \theta_{13} < 3.8 \times 10^{-5}$ for assumed i.h.

If the “true” mixing angle is large, we are able to distinguish among hierarchies. Assuming the “true” hierarchy is normal and the value of θ_{13} is large (n.h.-L), we could put a lower limit on the θ_{13} angle ($\sin^2 \theta_{13} > 2.1 \times 10^{-4}$) for an assumed n.h. The assumed i.h. is excluded. The same is possible for the case of inverted hierarchy being the limit $\sin^2 \theta_{13} > 2.3 \times 10^{-4}$. The assumed n.h. is excluded.

We illustrate the importance of the neutral current events. If we do not include the information given by NC events, we loose sensitivity in the large mixing angle cases. The limit in the case of n.h.-L can be set only at the level of 1σ and no limit can be determined for i.h.-L. Moreover, without NC events, i.h.-L could be misidentified as n.h.-S.

5.1.2 Supernova scenario II and 100 kton detector

If we consider the supernova scenario II, we see that the results of the fit obtained with a 3 kton detector are quite marginal. In this case the average energies of ν_x are very close to those ν_e and $\bar{\nu}_e$. It is impossible to distinguish among hierarchies and no bounds on the mixing angle can be set. Only a lower limit is obtained for the case of n.h.-L ($\sin^2 \theta_{13} > 6.2 \times 10^{-5}$).

In order to be sensitive to the oscillation parameters even in the scenario II we consider a 100 kton detector (see Figure 7). In this case the sensitivity to the parameters is almost the same for scenarios I and II. We can appreciate that the neutral current events are crucial even with such a big detector. They are specially important to discriminate the large mixing angle regions if the average energies of the neutrinos are close, as we already discussed.

5.2 Intermediate value of the mixing angle

If the θ_{13} mixing angle is in the intermediate range ($2 \times 10^{-6} < \sin^2 \theta_{13} < 3 \times 10^{-4}$), maximal sensitivity to the angle is achieved and measurements of the value are possible in this region, since one expects an energy dependent effect in the relevant energy region of the supernova neutrinos (see e.g. Ref. [11]).

If we consider a mixing angle $\sin^2 \theta_{13} = 10^{-4}$, the χ^2 fit gives the results shown in figure 8. True normal (n.h.-i) and inverted (i.h.-i) hierarchies for true $\sin^2 \theta_{13} = 10^{-4}$ and the two supernova scenarios are studied. Solid lines correspond to the contribution of the four neutrino detection channels while dashed lines only consider elastic and CC events. The one- and two- sigma levels are shown by horizontal lines.

A determination of the angle is possible at 1σ level for scenario I with a 3 kton detector considering all neutrino processes. We obtain the following 1σ intervals and mass hierarchies for a 3 kton detector:

$$5.8 \times 10^{-5} < \sin^2 \theta_{13} < 1.9 \times 10^{-4} \quad (\text{assumed n.h.}) \quad (17)$$

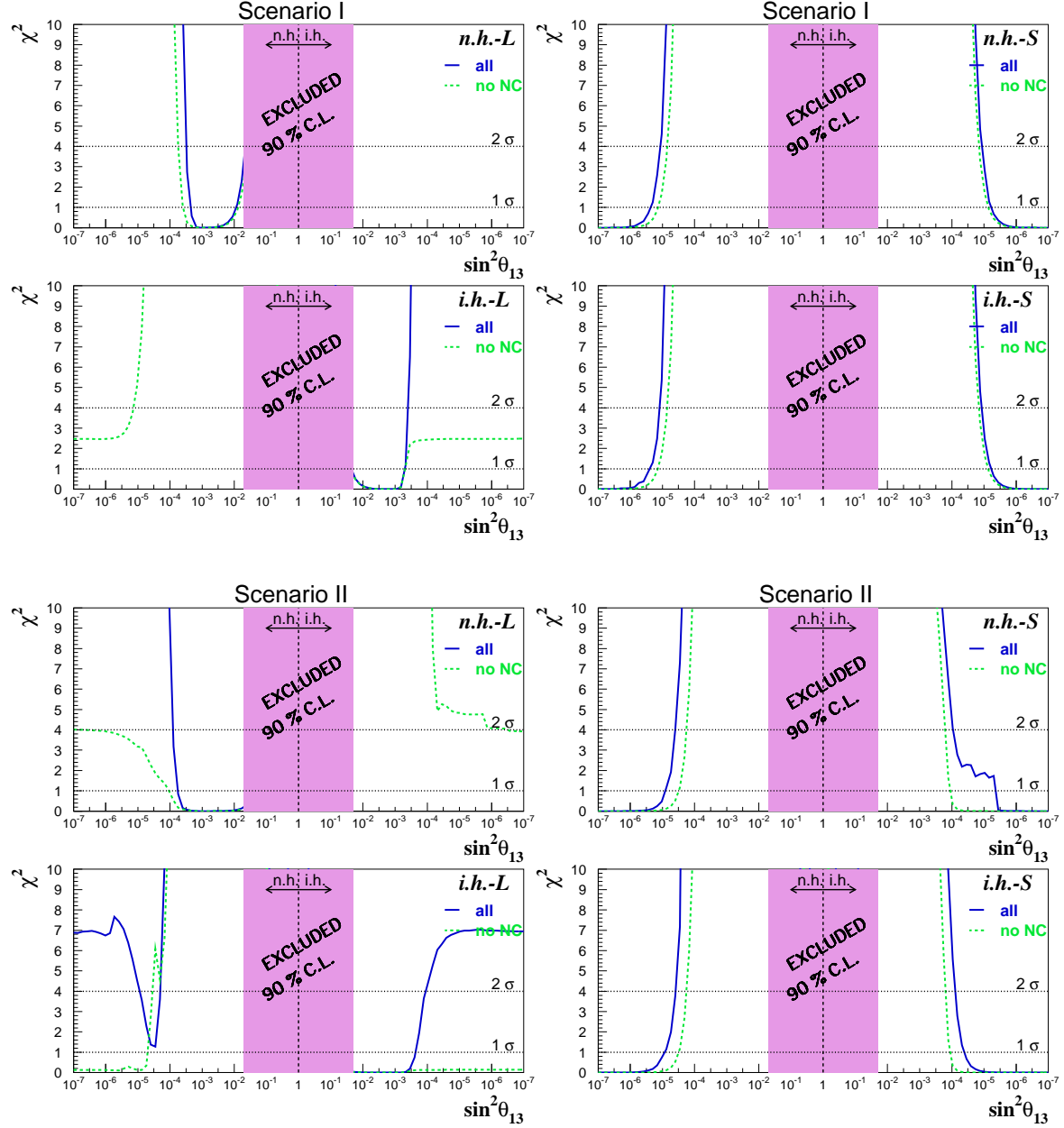


Figure 7: **Extreme mixing angle cases and 100 kton detector:** χ^2 value of the fit as a function of $\sin^2 \theta_{13}$ for a 100 kton detector. Curves on the left (right) part of every plot correspond to the results of the fit under the assumption of a normal (inverted) hierarchy. Four limiting oscillation scenarios (n.h.-L, n.h.-S, i.h.-L, i.h.-S) are considered as “true” and the reference values of the supernova parameters correspond to scenario I (top) and II (bottom). Solid curves are computed using the information of the four supernova neutrino detection processes and the dashed line does not take into account NC events.

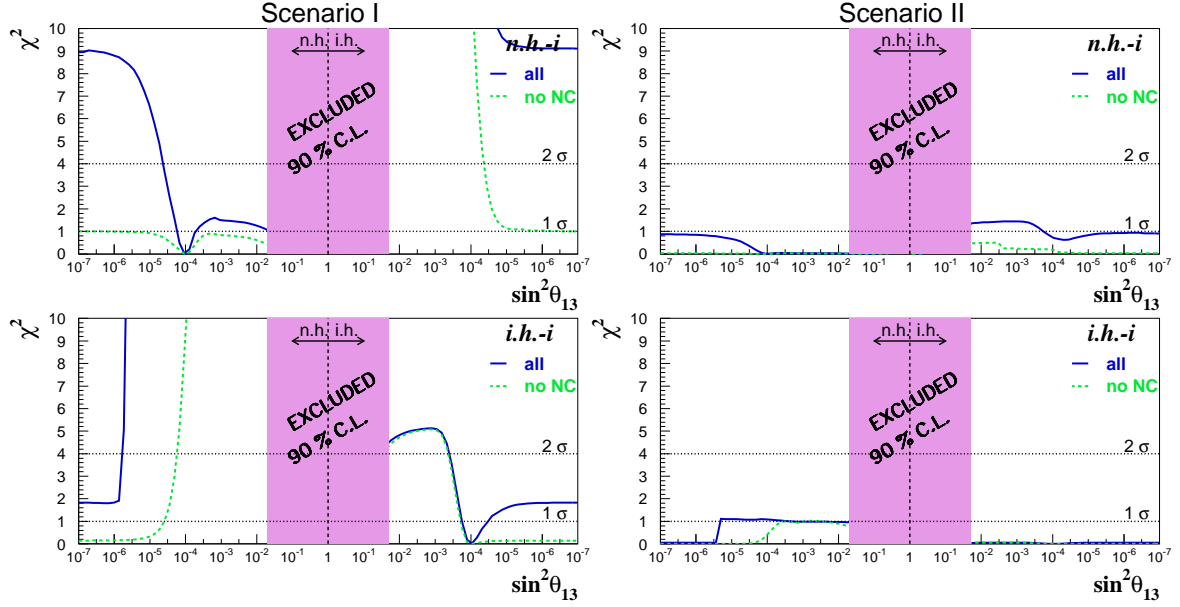


Figure 8: **Intermediate mixing angle region** ($\sin^2 \theta_{13} = 10^{-4}$): χ^2 value of the fit as a function of $\sin^2 \theta_{13}$ for a 3 kton detector. Curves on the left (right) part of every plot correspond to results of the fit for assumed normal (inverted) hierarchy. Two true oscillation scenarios are considered (n.h. and i.h.) and the true values of the supernova parameters correspond to scenario I (left) and II (right). Solid curves are computed using the information of the four supernova neutrino detection processes and the dashed line does not take into account NC events.

$$3.3 \times 10^{-5} < \sin^2 \theta_{13} < 1.8 \times 10^{-4} \quad (\text{assumed } i.h.) \quad (18)$$

The wrong hierarchies are excluded in both cases.

However, the statistics achieved with such a mass are not enough to put any constraint on the θ_{13} angle if the supernova parameters correspond to scenario II. Figure 9 compares the determination of the $\sin^2 \theta_{13}$ parameter using a 3 and a 100 kton detector. The χ^2 of the fit is plotted as a function of the $\sin^2 \theta_{13}$ value.

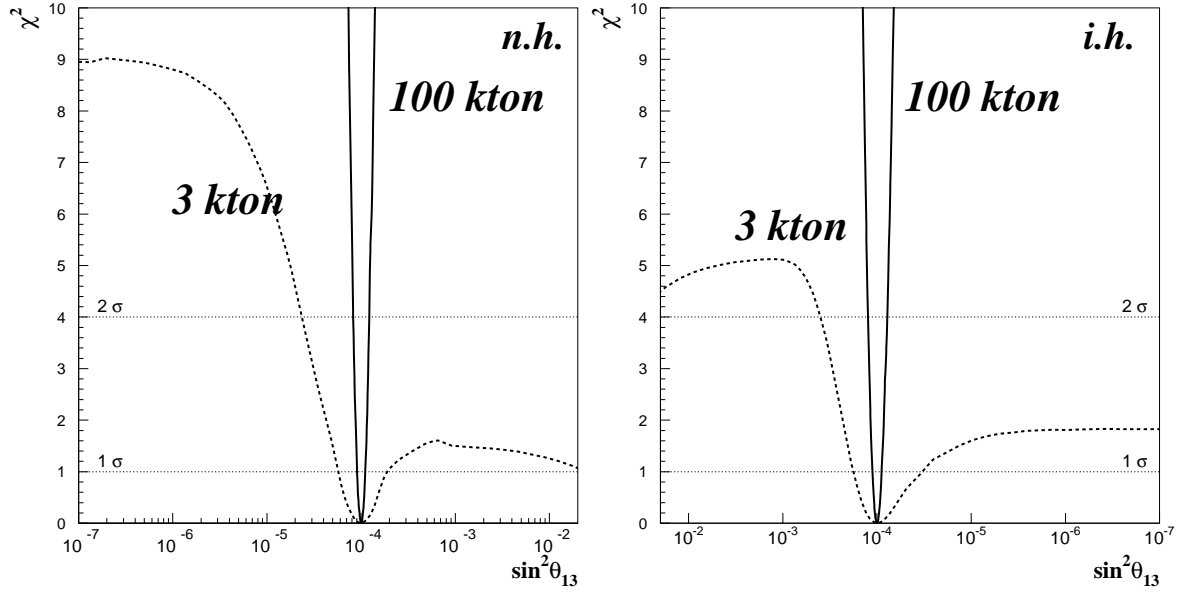


Figure 9: Determination of the $\sin^2 \theta_{13}$ parameter in the intermediate region. We have considered as “true” values $\sin^2 \theta_{13} = 10^{-4}$, normal (left) and inverted (right) hierarchies and the supernova parameters of scenario I. The solid curve corresponds to the results of the χ^2 fit obtained with a 100 kton detector and dashed line shows the contribution of a 3 kton. The one- and two- sigma levels are shown by horizontal lines.

If we consider a 100 kton detector, much more statistically accurate measurements can be performed at 1σ and 2σ levels:

$$9.1(8.1) \times 10^{-5} < \sin^2 \theta_{13} < 1.1(1.3) \times 10^{-4} \quad 1\sigma(2\sigma) \quad (\text{assumed } n.h.) \quad (19)$$

$$8.9(7.4) \times 10^{-5} < \sin^2 \theta_{13} < 1.1(1.3) \times 10^{-4} \quad 1\sigma(2\sigma) \quad (\text{assumed } i.h.) \quad (20)$$

The wrong hierarchies are excluded in both cases.

The precision on the measurement of the mixing angle will depend on the exact value of θ_{13} . Considering different reference values in the intermediate region, Figure 10 shows the superposition of different determinations of the $\sin^2 \theta_{13}$ parameter, for the cases of true normal and inverted hierarchies normalized to a 3 kton detector. The angle can be measured at 1σ in both cases.

The estimated limits and ranges of $\sin^2 \theta_{13}$ are summarized in table 5 for true normal and inverted hierarchies. If the $\sin^2 \theta_{13}$ angle is between $\approx (4 \times 10^{-5} - 1 \times 10^{-4})$ (n.h.) or $\approx (7 \times 10^{-5} - 3 \times 10^{-4})$ (i.h.), it could be constrained in a certain range. Otherwise, upper or lower limits on its value can be set.

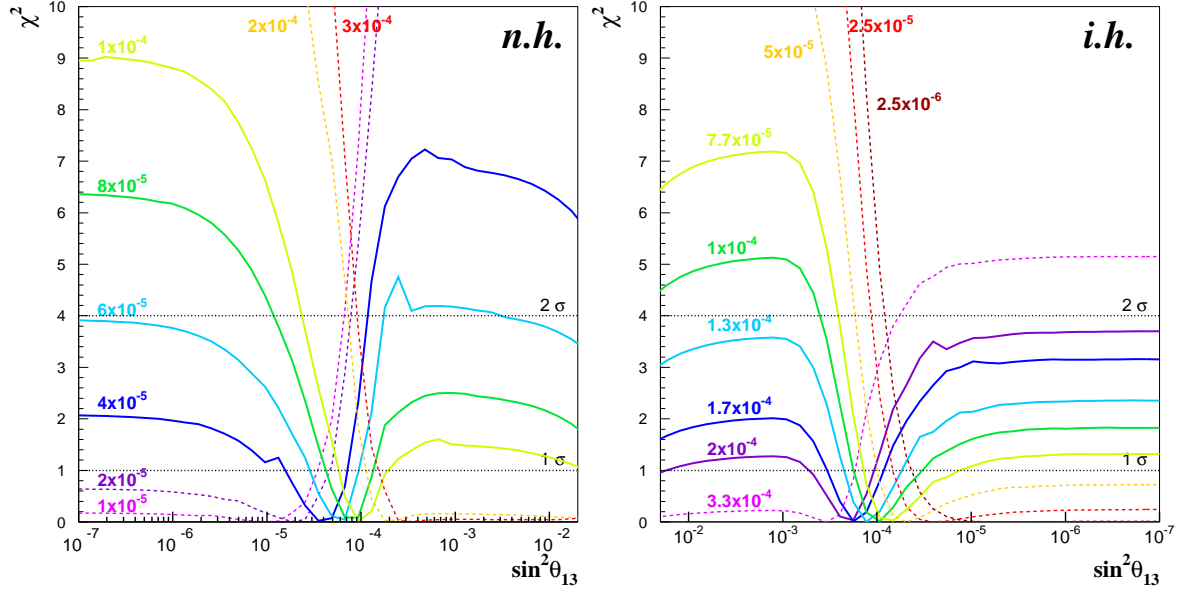


Figure 10: Determination of the $\sin^2 \theta_{13}$ parameter in the intermediate region with a 3 kton detector. We have considered different “true” values for $\sin^2 \theta_{13}$ and normal and inverted hierarchies. The reference supernova parameters correspond to scenario I. The one- and two-sigma levels are shown by horizontal lines.

3 kton detector	
“True” value $\sin^2 \theta_{13}$	Limit or range of $\sin^2 \theta_{13}$ at 1σ level
True n.h.	n.h. assumed
$1. \times 10^{-5}$	$\sin^2 \theta_{13} < 3.4 \times 10^{-5}$
$2. \times 10^{-5}$	$\sin^2 \theta_{13} < 4.6 \times 10^{-5}$
$4. \times 10^{-5}$	$1.6 \times 10^{-5} < \sin^2 \theta_{13} < 7.2 \times 10^{-5}$
$6. \times 10^{-5}$	$2.8 \times 10^{-5} < \sin^2 \theta_{13} < 9.4 \times 10^{-5}$
$8. \times 10^{-5}$	$4.2 \times 10^{-5} < \sin^2 \theta_{13} < 1.3 \times 10^{-4}$
$1. \times 10^{-4}$	$5.8 \times 10^{-5} < \sin^2 \theta_{13} < 1.9 \times 10^{-4}$
$2. \times 10^{-4}$	$\sin^2 \theta_{13} > 1.1 \times 10^{-4}$
$3. \times 10^{-4}$	$\sin^2 \theta_{13} > 1.5 \times 10^{-4}$
True i.h.	i.h. assumed
2.5×10^{-6}	$\sin^2 \theta_{13} < 4.0 \times 10^{-5}$
2.5×10^{-5}	$\sin^2 \theta_{13} < 6.8 \times 10^{-5}$
5.0×10^{-5}	$\sin^2 \theta_{13} < 9.9 \times 10^{-5}$
7.7×10^{-5}	$1.3 \times 10^{-5} < \sin^2 \theta_{13} < 1.4 \times 10^{-4}$
1.0×10^{-4}	$3.3 \times 10^{-5} < \sin^2 \theta_{13} < 1.8 \times 10^{-4}$
1.3×10^{-4}	$5.4 \times 10^{-5} < \sin^2 \theta_{13} < 2.2 \times 10^{-4}$
1.7×10^{-4}	$8.5 \times 10^{-5} < \sin^2 \theta_{13} < 3.4 \times 10^{-4}$
2.0×10^{-4}	$1.1 \times 10^{-4} < \sin^2 \theta_{13} < 5.3 \times 10^{-4}$
3.3×10^{-4}	$\sin^2 \theta_{13} > 1.7 \times 10^{-4}$

Table 5: Estimated limit on the θ_{13} mixing angle at 1σ level for different “true” values of the angle and mass hierarchies in the intermediate range.

6 Study of the supernova parameters assuming that the oscillation parameters are known

In this section we study the information about the astrophysical parameters that can be extracted from the detection of supernova neutrinos assuming that the oscillation parameters $\sin^2 \theta_{13}$ and the mass hierarchy have been determined from terrestrial experiments, essentially from long-baseline experiments.

Considering the range of sensitivity of θ_{13} of future accelerator experiments (see e.g. [20]), we can study two cases:

1. **If θ_{13} angle is measured by long-baseline experiments:** If the true value of the θ_{13} angle is large ($\sin^2 \theta_{13} \gtrsim 10^{-3}$) then future superbeams should be able to measure it (see e.g. [20]). We assume that the angle will be determined with a precision of 10%. Therefore, we study how well we can constrain the supernova parameters under the external constraint $\sin^2 \theta_{13} = 10^{-3} \pm 10^{-4}$, considering that the mass hierarchy is also known.
2. **If an upper bound on θ_{13} angle is set by long-baseline experiments:** If the angle is very small, then future long-baseline experiments might not have the possibility to measure this angle and will only place an upper limit on the value. As a second example, we consider that the limit $\sin^2 \theta_{13} < 10^{-4}$ has been set and we investigate the consequences of this limit into the determination of the supernova parameters.

6.1 If θ_{13} angle is measured by long-baseline experiments

We assume that the value of the true θ_{13} mixing angle has been determined by long-baseline experiments to be $\sin^2 \theta_{13} = 10^{-3} \pm 10^{-4}$ and we study the cases of true normal and inverted hierarchies. We will compare the precisions in the determinations of the supernova parameters with a 3 and 100 kton detectors. In the fits, we let free the supernova parameters (E_B , $\langle E_{\nu_e} \rangle$, $\langle E_{\bar{\nu}_e} \rangle$, $\langle E_{\nu_x} \rangle$, L_e/L_x) and we perform a χ^2 minimization in order to obtain the allowed regions in different 1D parameter regions and 2D parameter planes. The expected accuracies at 90% C.L. to be achieved with a 3 and 100 kton detectors are summarized in Table 6.

Figure 11 shows on the top the χ^2 value of the fit as a function of the supernova parameters for a 3 kton detector for true normal hierarchy. Figures 12 correspond to the inverted hierarchy case. The bottom plots are the 68%, 90% and 99% C.L. allowed regions for the astrophysical parameters with a 100 kton detector. The crosses on the plots indicate the values of the parameters taken as reference for the fit, which correspond to scenario I.

The plots L_e/L_x vs $\langle E_{\nu} \rangle$ show the luminosity of every flavor as a function of its average energy. We see that with the statistics given by the 3 kton detector is not possible put any constraint on the $\langle E_{\nu_e} \rangle$ and $\langle E_{\bar{\nu}_e} \rangle$ energies or on L_e/L_x . However, the $\langle E_{\nu_x} \rangle$ energy can be determined very precisely. The accuracy that we can achieve at 90% C.L. is $\Delta \langle E_{\nu_x} \rangle / \langle E_{\nu_x} \rangle \sim 3\%$.

The plot E_B vs L_e/L_x shows the strong correlation between these two variables. Using a 100 kton detector, all the variables can be determined in a certain range. The best results are obtained for $\langle E_{\nu_x} \rangle$ because we are considering the large θ_{13} mixing angle. In this case the

With constraint $\sin^2 \theta_{13} = 10^{-3} \pm 10^{-4}$ from terrestrial experiment							
Detector mass	True hierarchy	SN scen.	$\frac{\Delta \langle E_{\nu_e} \rangle}{\langle E_{\nu_e} \rangle}$	$\frac{\Delta \langle E_{\bar{\nu}_e} \rangle}{\langle E_{\bar{\nu}_e} \rangle}$	$\frac{\Delta \langle E_{\nu_x} \rangle}{\langle E_{\nu_x} \rangle}$	$\frac{\Delta E_B}{E_B}$	$\frac{\Delta (L_e/L_x)}{(L_e/L_x)}$
3 kton	n.h.	I	–	–	$\sim 3\%$	$\sim 23\%$	–
3 kton	i.h.	I	$\sim 46\%$	–	$\sim 7\%$	$\sim 17\%$	$\sim 60\%$
3 kton	n.h.	II	–	$\sim 26\%$	$\sim 4\%$	$\sim 28\%$	–
3 kton	i.h.	II	–	$\sim 36\%$	$\sim 19\%$	$\sim 20\%$	–
100 kton	n.h.	I	$\sim 14\%$	$\sim 4\%$	$< 1\%$	$\sim 2\%$	$\sim 11\%$
100 kton	i.h.	I	$\sim 5\%$	$\sim 9\%$	$\sim 1\%$	$\sim 2\%$	$\sim 9\%$
100 kton	n.h.	II	$\sim 9\%$	$\sim 3\%$	$< 1\%$	$\sim 4\%$	$\sim 12\%$
100 kton	i.h.	II	$\sim 6\%$	$\sim 6\%$	$\sim 1\%$	$\sim 2\%$	$\sim 32\%$

Table 6: Expected accuracies at 90% C.L. in the determination of the supernova parameters using the neutrinos measured with a 3 kton and a 100 kton detector. We have assumed that the mass hierarchy is known and the θ_{13} mixing angle has been measured by long-baseline experiments, being equal to $\sin^2 \theta_{13} = 10^{-3} \pm 10^{-4}$. Supernova scenarios I and II are tested.

ν_e 's have oscillated into ν_μ 's and ν_τ 's (so ν_x 's) and vice versa. Therefore, the most important reaction on argon ($\nu_e \text{CC}$) will be mainly sensitive to the original $\langle E_{\nu_x} \rangle$.

In the inverted hierarchy case, a fraction of the ν_e flux arrives at the detector hence in this case we are sensitive to the $\langle E_{\nu_e} \rangle$ energy and a bit less to $\langle E_{\nu_x} \rangle$, but both variables can be estimated with accuracies of $\sim 46\%$ and $\sim 7\%$, respectively, for a 3 kton detector.

If we consider true values those given by scenario II (see table 1), the corresponding results for the χ^2 fit are presented in figures 13 (n.h.) and 14 (i.h.). For the normal hierarchy case we see that results are quite similar to those obtained for scenario I. Only the $\langle E_{\nu_x} \rangle$ parameter can be measured with a 3 kton detector. However, the inverted hierarchy case shows a worse situation. The ν_e and ν_x average energies are closer for scenario II and it makes more difficult the determination of a region in the plane ($\langle E_{\nu_e} \rangle$, $\langle E_{\nu_x} \rangle$).

For a 100 kton detector, scenarios I and II give quite similar results except for the L_e/L_x parameter in the case of i.h., which is worse determined for scenario II ($\sim 32\%$) than for scenario I ($\sim 9\%$) (see table 6).

6.2 If an upper bound on θ_{13} angle is set by long-baseline experiments

Another possibility is that future long-baseline neutrino experiments will not be sensitive enough to measure $\sin^2 \theta_{13}$ and will place an upper limit on its value. Assuming the limit $\sin^2 \theta_{13} < 10^{-4}$, we study the possible determination of the supernova parameters.

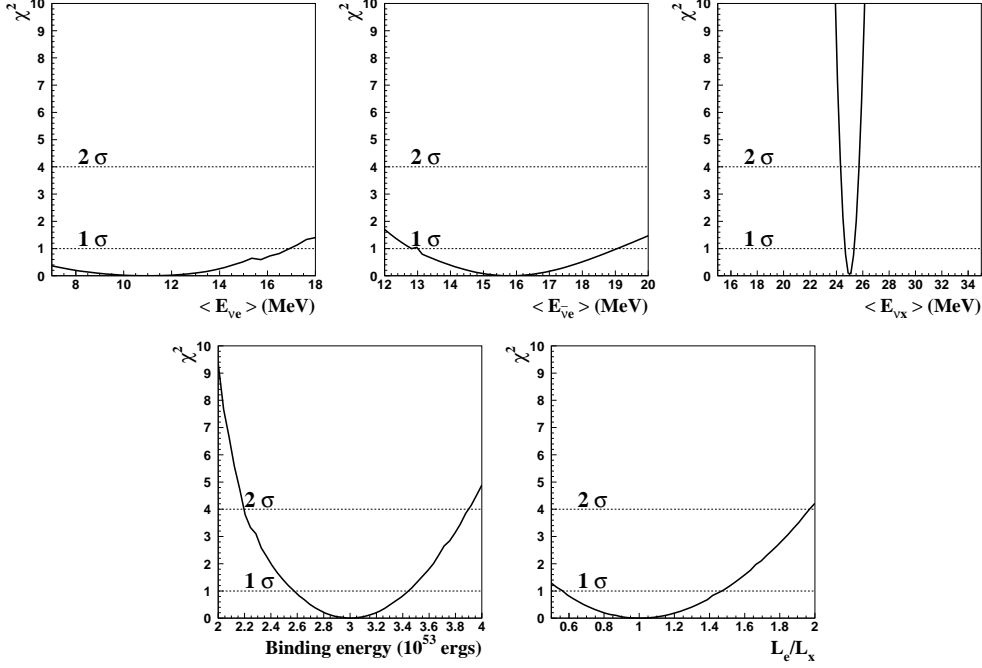
In this case the large mixing angle region for both hierarchies is excluded and we only have the possibility that the θ_{13} angle be in the intermediate (n.h.-i or i.h.-i) or in the small (n.h.-S or i.h.-S) mixing angle regions.

Putting the condition of $\sin^2 \theta_{13} < 10^{-4}$ and fixing the mass hierarchy, we perform a χ^2 minimization letting at each step all variables free, included the θ_{13} angle. The upper bound on the θ_{13} angle is inserted as an appropriate term in the χ^2 function. We study two cases for the “true” data: normal and inverted hierarchy.

Table 7 shows the expected accuracies at 90% C.L. in the determination of the supernova

$$\sin^2 \theta_{13} = 10^{-3} \pm 10^{-4} \text{ and n.h.}$$

3 kton LAr



100 kton LAr

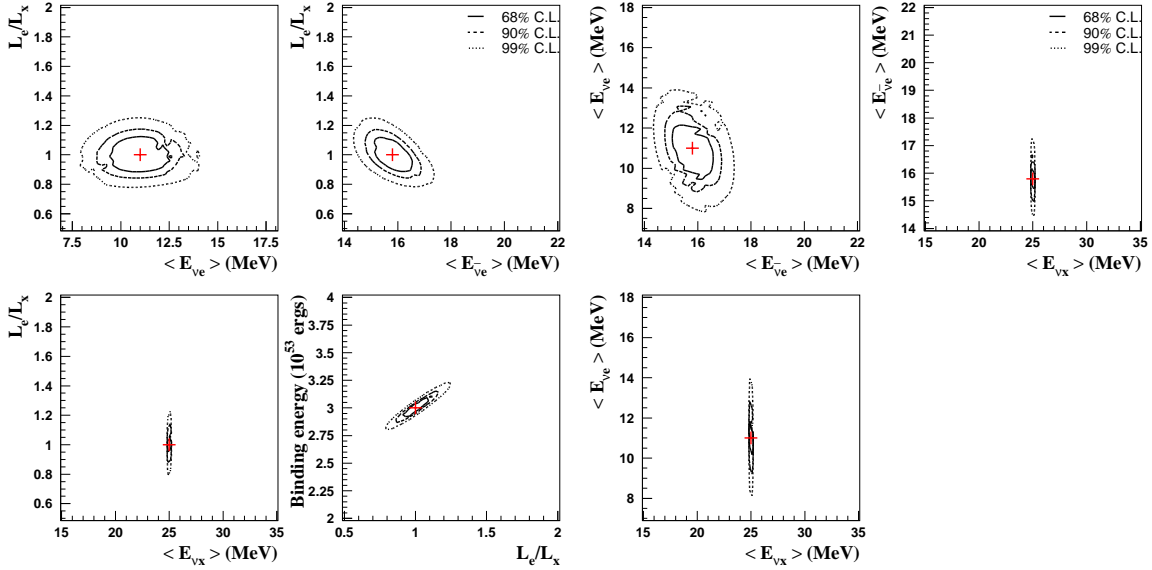
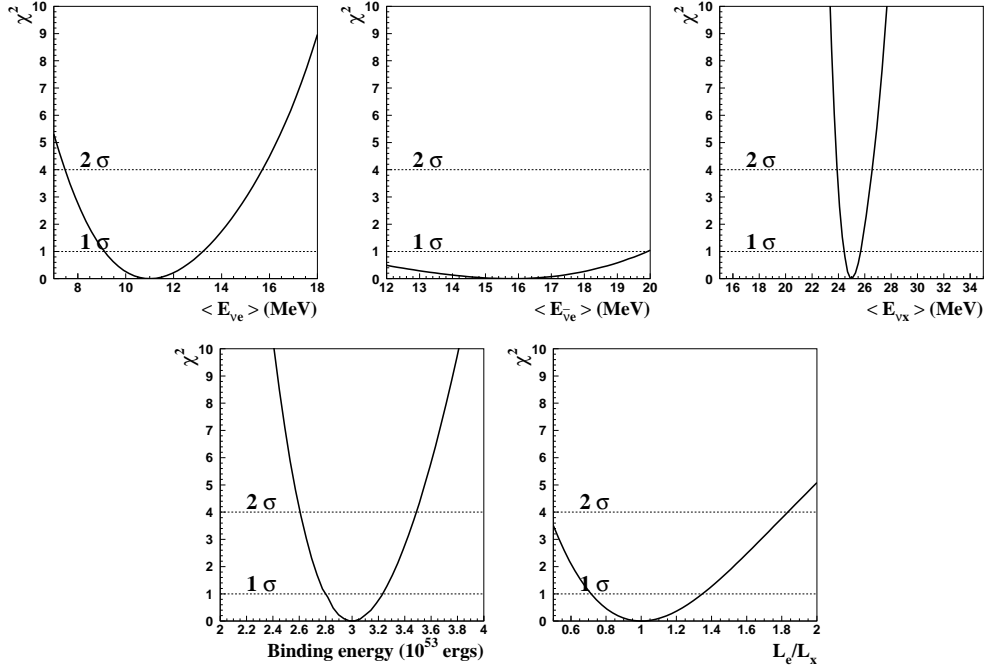


Figure 11: (Top) χ^2 value of the fit as a function of the supernova parameters for a 3 kton detector, assuming that the θ_{13} mixing angle has been measured with a precision of 10% ($\sin^2 \theta_{13} = 10^{-3} \pm 10^{-4}$) and the mass hierarchy is normal ($\Delta m_{31}^2 > 0$). (Bottom) 68%, 90% and 99% C.L. allowed regions for the supernova parameters with a 100 kton detector. Crosses indicate the value of the parameters for the best fits.

$$\sin^2 \theta_{13} = 10^{-3} \pm 10^{-4} \text{ and i.h.}$$

3 kton LAr



100 kton LAr

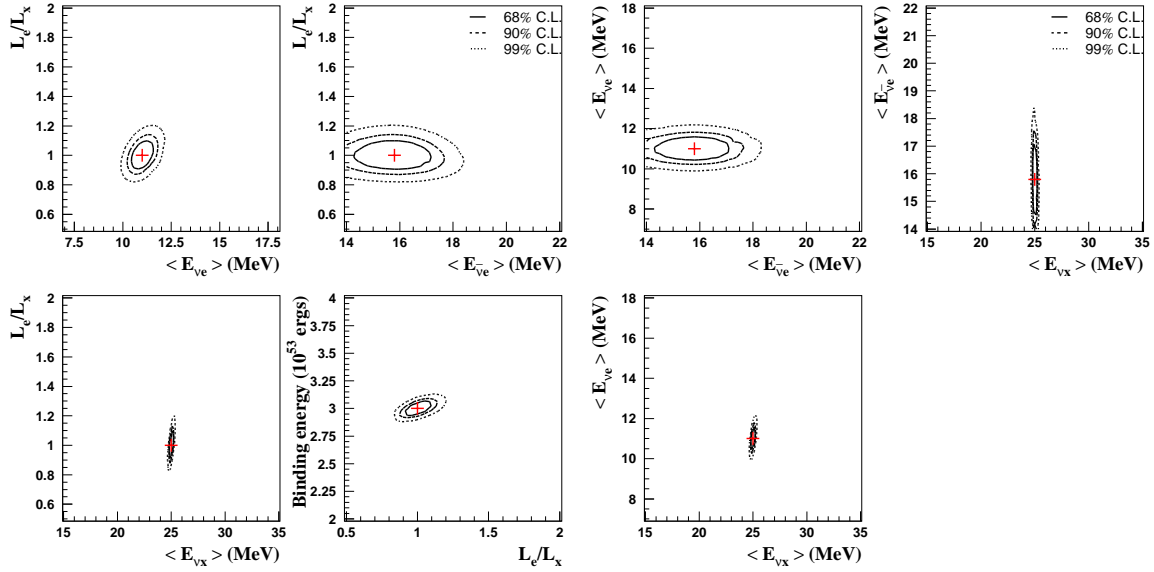
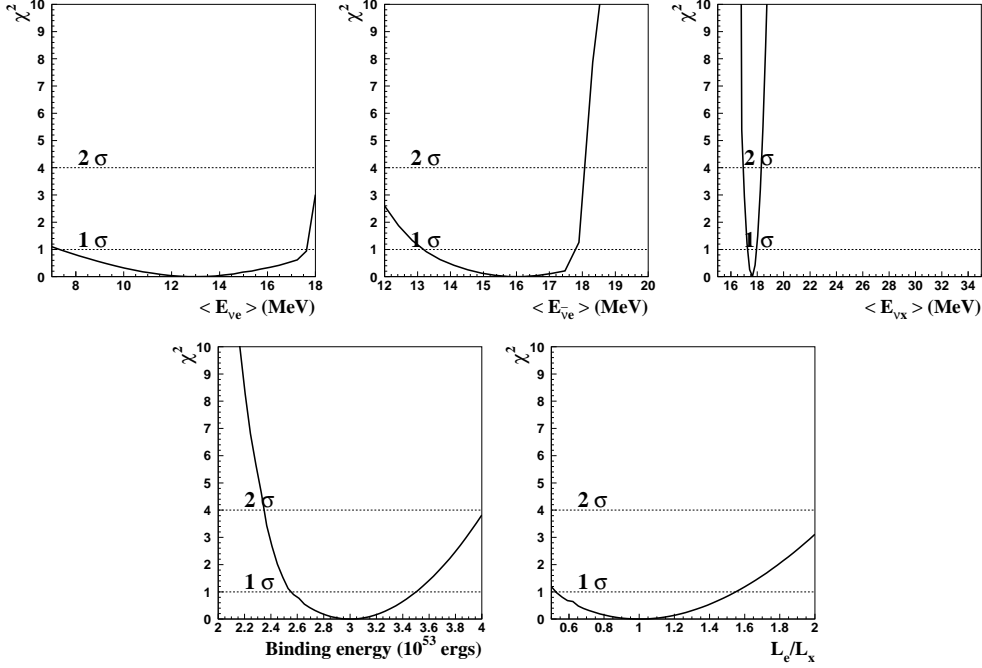


Figure 12: (Top) χ^2 value of the fit as a function of the supernova parameters for a 3 kton detector, assuming that the θ_{13} mixing angle has been measured with a precision of 10% ($\sin^2 \theta_{13} = 10^{-3} \pm 10^{-4}$) and the mass hierarchy is inverted ($\Delta m_{31}^2 < 0$). (Bottom) 68%, 90% and 99% C.L. allowed regions for the supernova parameters with a 100 kton detector. Crosses indicate the value of the parameters for the best fits.

$$\sin^2 \theta_{13} = 10^{-3} \pm 10^{-4} \text{ and n.h. (scen II)}$$

3 kton LAr



100 kton LAr

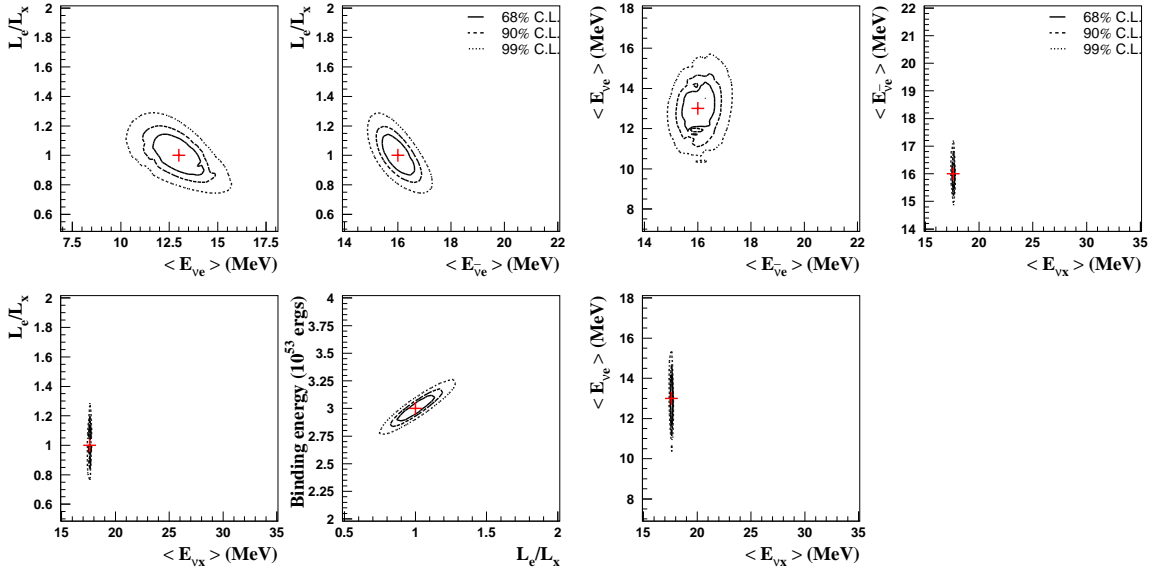
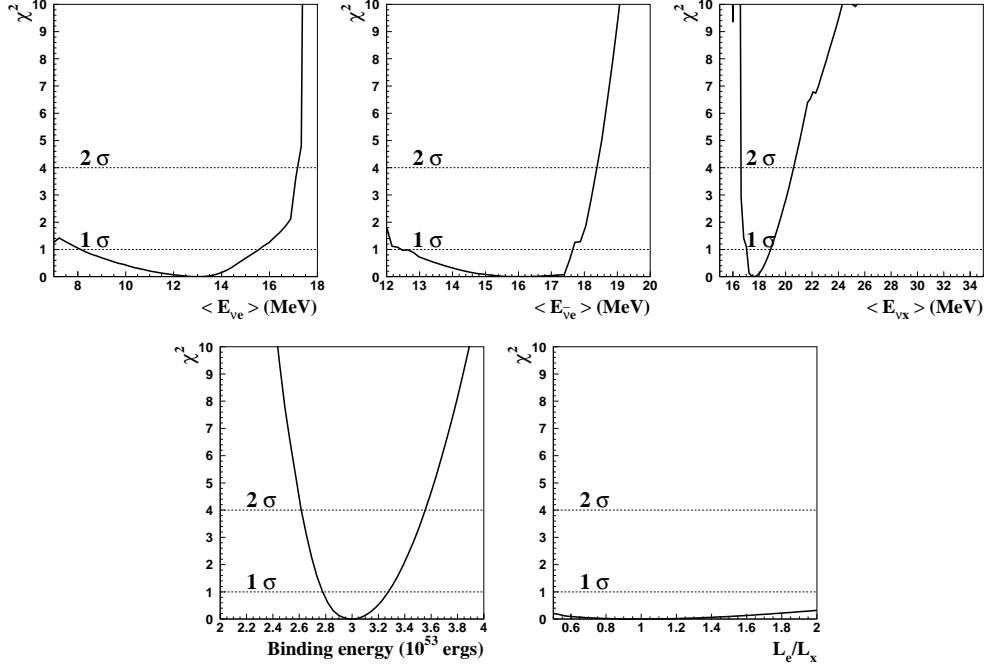


Figure 13: (Top) χ^2 value of the fit as a function of the supernova parameters for a 3 kton detector, assuming that the θ_{13} mixing angle has been measured with a precision of 10% ($\sin^2 \theta_{13} = 10^{-3} \pm 10^{-4}$) and the mass hierarchy is normal ($\Delta m_{31}^2 > 0$). The reference values taken for the neutrino average energies are the ones of scenario II (see table 1). (Bottom) 68%, 90% and 99% C.L. allowed regions for the supernova parameters with a 100 kton detector. Crosses indicate the value of the parameters for the best fits.

$$\sin^2 \theta_{13} = 10^{-3} \pm 10^{-4} \text{ and i.h. (scen II)}$$

3 kton LAr



100 kton LAr

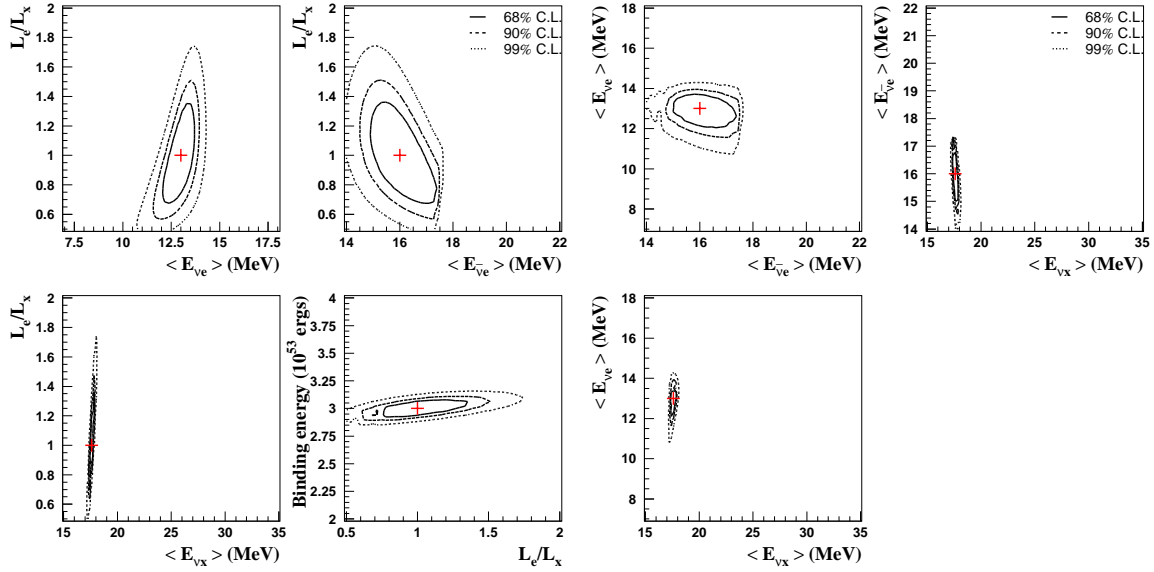


Figure 14: (Top) χ^2 value of the fit as a function of the supernova parameters for a 3 kton detector, assuming that the θ_{13} mixing angle has been measured with a precision of 10% ($\sin^2 \theta_{13} = 10^{-3} \pm 10^{-4}$) and the mass hierarchy is inverted ($\Delta m_{31}^2 < 0$). The reference values taken for the neutrino average energies are the ones of scenario II (see table 1). (Bottom) 68%, 90% and 99% C.L. allowed regions for the supernova parameters with a 100 kton detector. Crosses indicate the value of the parameters for the best fits.

parameters for 3 and 100 kton detectors and supernova scenarios I and II.

With constraint $\sin^2 \theta_{13} < 10^{-4}$ from terrestrial experiment							
Detector mass	True hierarchy	SN scen.	$\frac{\Delta \langle E_{\nu_e} \rangle}{\langle E_{\nu_e} \rangle}$	$\frac{\Delta \langle E_{\bar{\nu}_e} \rangle}{\langle E_{\bar{\nu}_e} \rangle}$	$\frac{\Delta \langle E_{\nu_x} \rangle}{\langle E_{\nu_x} \rangle}$	$\frac{\Delta E_B}{E_B}$	$\frac{\Delta(L_e/L_x)}{(L_e/L_x)}$
3 kton	n.h.	I	$\sim 30\%$	$\sim 30\%$	$\sim 7\%$	$\sim 26\%$	–
3 kton	i.h.	I	$\sim 52\%$	$\sim 30\%$	$\sim 8\%$	$\sim 17\%$	–
3 kton	n.h.	II	–	$\sim 25\%$	$\sim 16\%$	$\sim 27\%$	–
3 kton	i.h.	II	–	$\sim 25\%$	$\sim 23\%$	$\sim 17\%$	–
100 kton	n.h.	I	$\sim 6\%$	$\sim 4\%$	$< 1\%$	$\sim 1\%$	$\sim 11\%$
100 kton	i.h.	I	$\sim 5\%$	$\sim 4\%$	$< 1\%$	$\sim 2\%$	$\sim 9\%$
100 kton	n.h.	II	$\sim 9\%$	$\sim 5\%$	$< 1\%$	$\sim 2\%$	$\sim 35\%$
100 kton	i.h.	II	$\sim 8\%$	$\sim 4\%$	$\sim 1\%$	$\sim 2\%$	$\sim 37\%$

Table 7: Expected accuracies at 90% C.L. in the determination of the supernova parameters using the neutrinos measured with a 3 kton and a 100 kton detector. We have assumed that the mass hierarchy is known and an upper limit on the mixing angle of $\sin^2 \theta_{13} < 10^{-4}$ has been set by long-baseline neutrino experiments. Supernova scenarios I and II are tested.

Figures 15 and 16 show on the top the χ^2 value of the fit as a function of the supernova parameters for a 3 kton detector considering that an upper limit on the value of θ_{13} has been set ($\sin^2 \theta_{13} < 10^{-4}$) and for normal or inverted mass hierarchy, respectively. The bottom plots are the allowed regions at 68%, 90% and 99% C.L. on different supernova parameters planes for a 100 kton detector. A value of $\sin^2 \theta_{13} = 10^{-7}$ was taken as reference for the fit, i.e. in the small mixing angle region. However, the fitted angle can be in both intermediate and small mixing angle regions. We have checked that if the “true” value of the angle is $\sin^2 \theta_{13} = 10^{-5}$, the results of the χ^2 fit are only slightly modified.

In this case the poor determination of the parameters obtained with 3 kttons indicates that statistics are not enough for providing good results. However, a 100 kton detector will solve these problems.

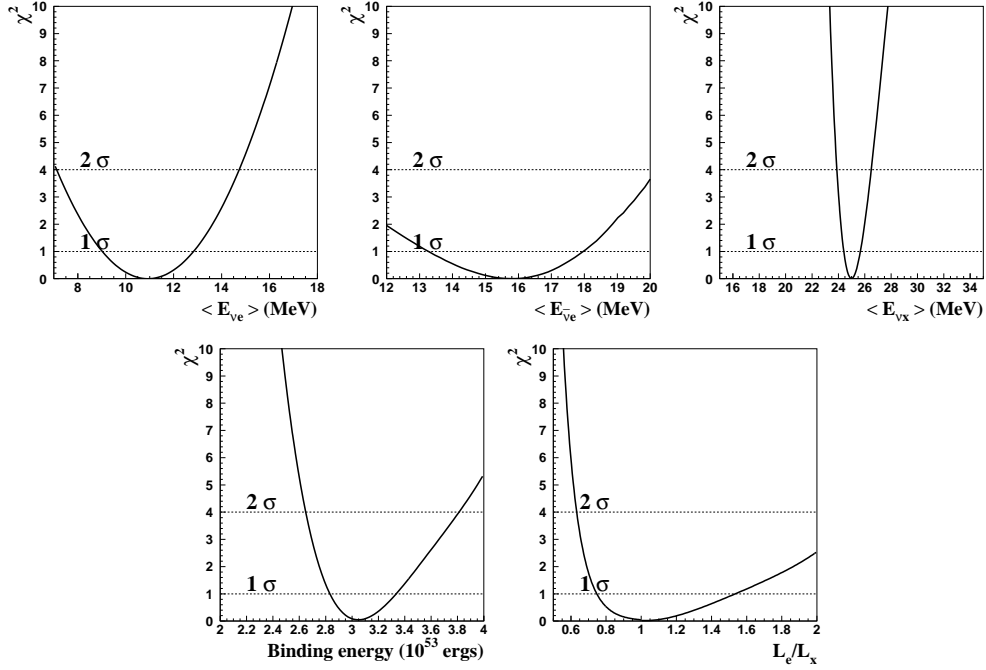
Normal and inverted hierarchy cases give different results because they depend on the value of the angle. For $\sin^2 \theta_{13} \lesssim 10^{-6}$ it is impossible to distinguish between both hierarchies. But if the angle is the intermediate region ($2 \times 10^{-6} < \sin^2 \theta_{13} < 3 \times 10^{-4}$) there is a dependence with the neutrino energy and the results depend on the particular value of θ_{13} . This is specially important in the n.h. case, where the survival probability changes with energy in the neutrino channel, which is the most sensitive for LAr detectors.

With a 100 kton detector, the expected accuracies are similar for normal and inverted hierarchies, as shown in table 7. Thanks to the high statistics available with a very massive detector, we can fit very precisely the data and the results are essentially equal for both mass hierarchies, as expected in the small θ_{13} region.

Considering the parameters of scenario II as reference values, the corresponding 2D allowed regions are presented in figures 17 and 18, for both mass hierarchies. In this case the determination of $\langle E_{\nu_e} \rangle$ and $\langle E_{\nu_x} \rangle$ is more complicated due to the non-hierarchical scenario. Likewise, L_e/L_x presents a big uncertainty even with a 100 kton detector.

$$\sin^2 \theta_{13} < 10^{-4} \text{ and n.h.}$$

3 kton LAr



100 kton LAr

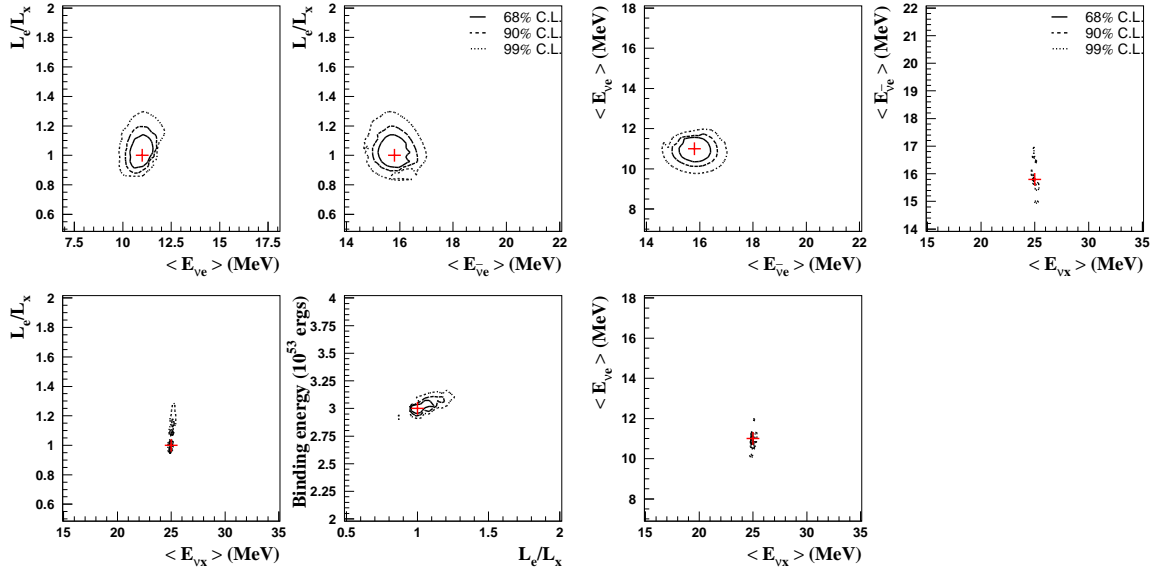
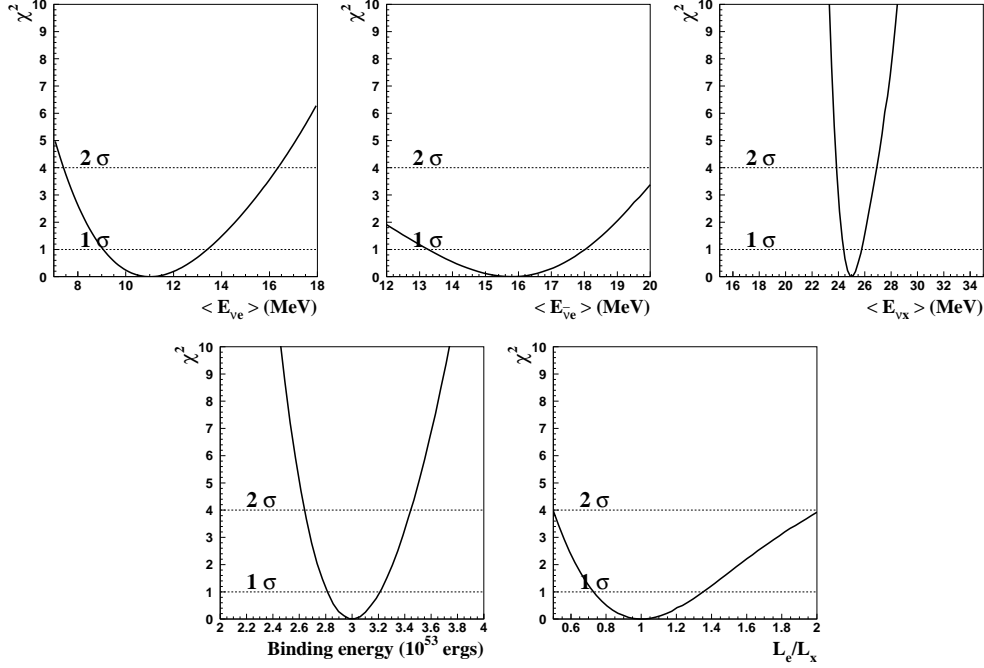


Figure 15: (Top) χ^2 value of the fit as a function of the supernova parameters for a 3 kton detector, assuming that an upper limit on the value of the θ_{13} mixing angle has been set ($\sin^2 \theta_{13} < 10^{-4}$) and the mass hierarchy is normal ($\Delta m_{31}^2 > 0$). (Bottom) 68%, 90% and 99% C.L. allowed regions for the supernova parameters with a 100 kton detector. Crosses indicate the value of the parameters for the best fits.

$$\sin^2 \theta_{13} < 10^{-4} \text{ and i.h.}$$

3 kton LAr



100 kton LAr

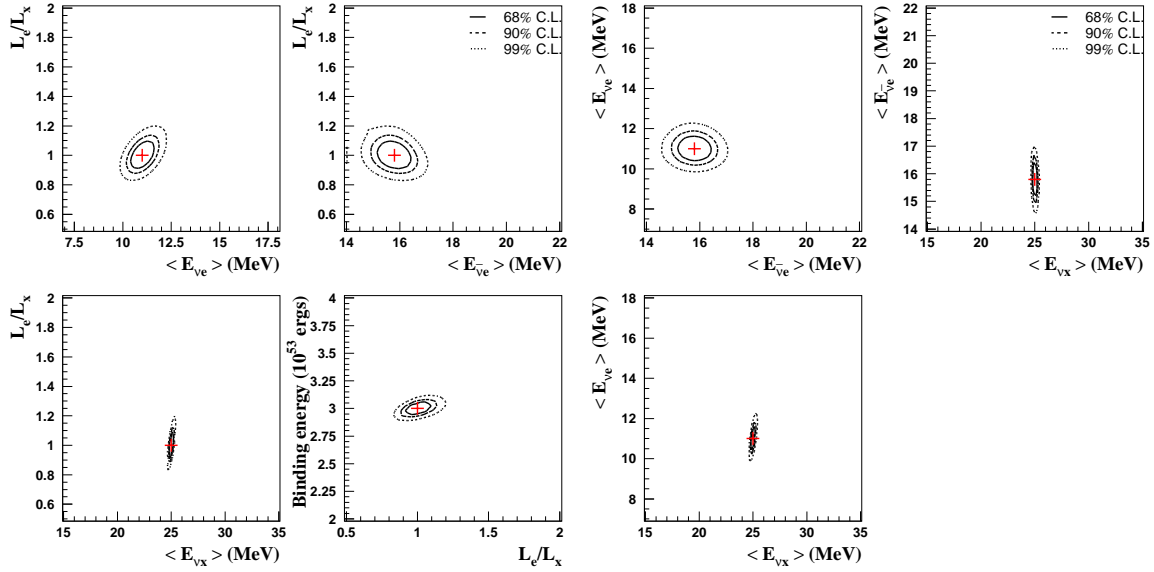
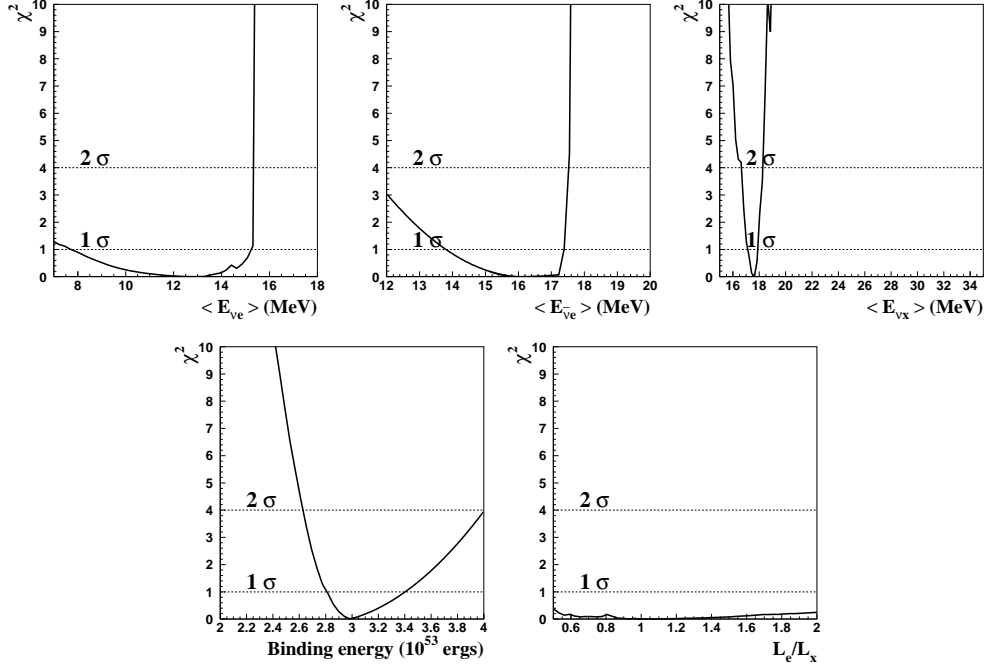


Figure 16: (Top) χ^2 value of the fit as a function of the supernova parameters for a 3 kton detector, assuming that an upper limit on the value of the θ_{13} mixing angle has been set ($\sin^2 \theta_{13} < 10^{-4}$) and the mass hierarchy is inverted ($\Delta m_{31}^2 < 0$). (Bottom) 68%, 90% and 99% C.L. allowed regions for the supernova parameters with a 100 kton detector. Crosses indicate the value of the parameters for the best fits.

$$\sin^2 \theta_{13} < 10^{-4} \text{ and n.h. (scen II)}$$

3 kton LAr



100 kton LAr

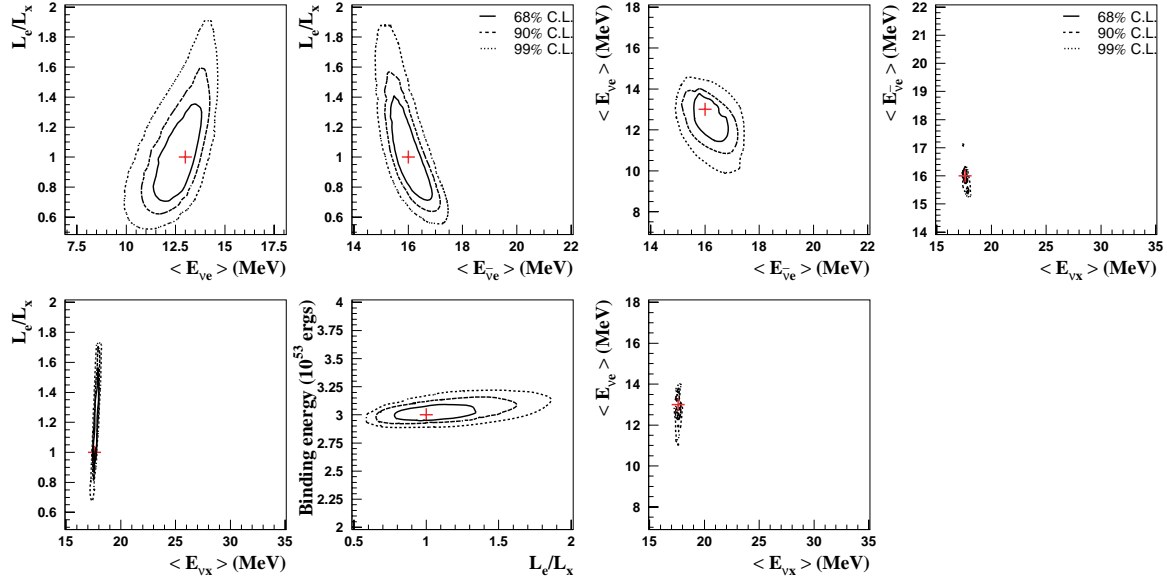
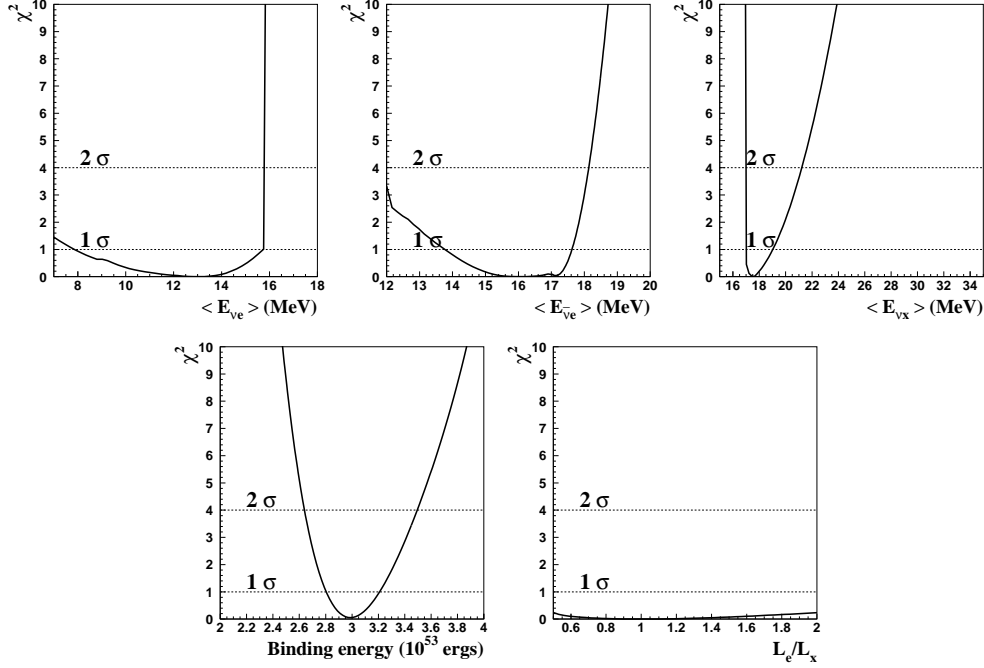


Figure 17: (Top) χ^2 value of the fit as a function of the supernova parameters for a 3 kton detector, assuming that an upper limit on the value of the θ_{13} mixing angle has been set ($\sin^2 \theta_{13} < 10^{-4}$) and the mass hierarchy is normal ($\Delta m_{31}^2 > 0$). The reference values taken for the neutrino average energies are the ones of scenario II (see table 1). (Bottom) 68%, 90% and 99% C.L. allowed regions for the supernova parameters with a 100 kton detector. Crosses indicate the value of the parameters for the best fits.

$$\sin^2 \theta_{13} < 10^{-4} \text{ and i.h. (scen II)}$$

3 kton LAr



100 kton LAr

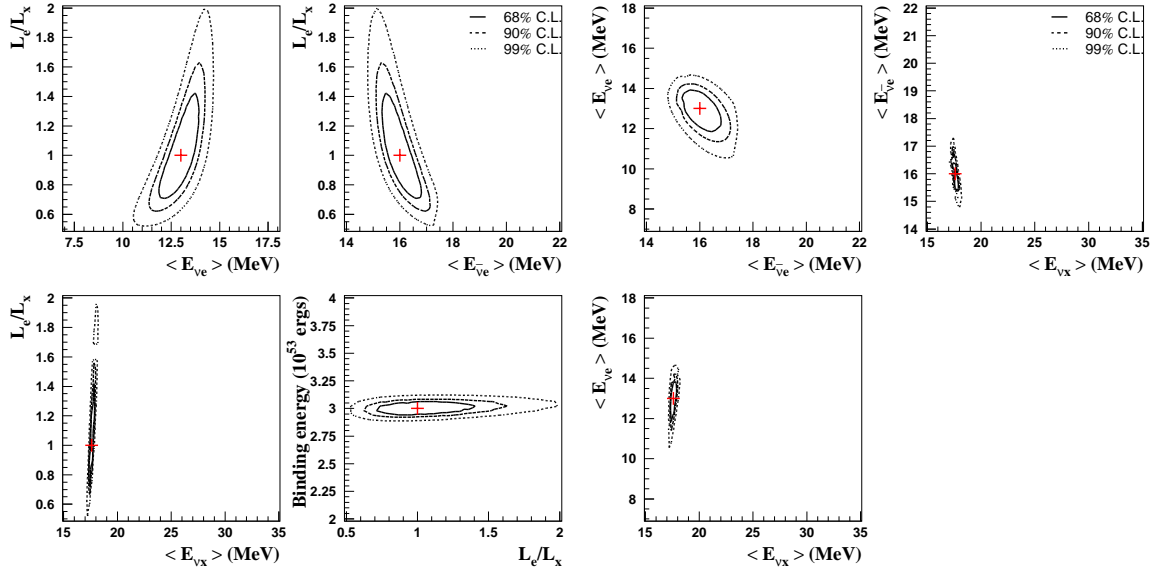


Figure 18: (Top) χ^2 value of the fit as a function of the supernova parameters for a 3 kton detector, assuming that an upper limit on the value of the θ_{13} mixing angle has been set ($\sin^2 \theta_{13} < 10^{-4}$) and the mass hierarchy is inverted ($\Delta m_{31}^2 < 0$). The reference values taken for the neutrino average energies are the ones of scenario II (see table 1). (Bottom) 68%, 90% and 99% C.L. allowed regions for the supernova parameters with a 100 kton detector. Crosses indicate the value of the parameters for the best fits.

7 Study of the supernova parameters without any knowledge on the neutrino oscillation parameters

We consider four cases as “true” values of the oscillation parameters: n.h.-L, i.h.-L, n.h.-S, i.h.-S. Without assuming any value of the mixing angle and mass hierarchy, we perform a χ^2 minimization letting all parameters $\{E_B, \langle E_{\nu_e} \rangle, \langle E_{\bar{\nu}_e} \rangle, \langle E_{\nu_x} \rangle, L_e/L_x, \sin^2 \theta_{13}, \text{sign}[\Delta m_{32}^2]\}$ freely vary and we study how well we can determine them in the case of a 100 kton detector. For the 3 kton detector, the results can be rescaled accordingly.

Figures 19 and 20 show the allowed regions at 68%, 90% and 99% C.L. of the oscillation and supernova parameters. The reference values of the parameters correspond to scenario I.

The results show that with large statistics it is possible to decouple the supernova and oscillations parameters and determine the parameters with high precision, as presented in Table 8. The expected accuracies at 90% C.L. are listed for every astrophysical parameter, supernova scenario and “true” oscillation case considered. The total binding energy (E_B) has an error 1–4%, the average energy of electron neutrinos $\langle E_{\nu_e} \rangle$ at the core is determined with an error 5–21%, the average energy of electron antineutrinos $\langle E_{\bar{\nu}_e} \rangle$ at the core, with an error 4–9%, the average energy of other (anti)neutrinos $\langle E_{\nu_x} \rangle$ at the core is determined with an error $\sim 1\%$, and the relative luminosities of the electron and non-electron flavor neutrinos L_e/L_x , with an error 9–37%. The errors with a 3 kton detector are roughly 6 times larger than those with a 100 kton detector, hence, many of the parameters would be poorly determined in this case.

100 kton detector. All parameters free.						
“True” osc. case	SN scen.	$\frac{\Delta \langle E_{\nu_e} \rangle}{\langle E_{\nu_e} \rangle}$	$\frac{\Delta \langle E_{\bar{\nu}_e} \rangle}{\langle E_{\bar{\nu}_e} \rangle}$	$\frac{\Delta \langle E_{\nu_x} \rangle}{\langle E_{\nu_x} \rangle}$	$\frac{\Delta E_B}{E_B}$	$\frac{\Delta (L_e/L_x)}{(L_e/L_x)}$
n.h.-L	I	$\sim 17\%$	$\sim 4\%$	$< 1\%$	$\sim 2\%$	$\sim 11\%$
i.h.-L	I	$\sim 5\%$	$\sim 9\%$	$< 1\%$	$\sim 2\%$	$\sim 9\%$
n.h.-S	I	$\sim 6\%$	$\sim 4\%$	$< 1\%$	$\sim 1\%$	$\sim 11\%$
i.h.-S	I	$\sim 5\%$	$\sim 4\%$	$< 1\%$	$\sim 2\%$	$\sim 9\%$
n.h.-L	II	$\sim 21\%$	$\sim 3\%$	$< 1\%$	$\sim 4\%$	$\sim 14\%$
i.h.-L	II	$\sim 6\%$	$\sim 9\%$	$\sim 1\%$	$\sim 2\%$	$\sim 34\%$
n.h.-S	II	$\sim 11\%$	$\sim 5\%$	$< 1\%$	$\sim 2\%$	$\sim 35\%$
i.h.-S	II	$\sim 8\%$	$\sim 4\%$	$\sim 1\%$	$\sim 2\%$	$\sim 37\%$

Table 8: Expected accuracies at 90% C.L. in the determination of the supernova parameters using the neutrinos measured with a 100 kton detector. No conditions on the θ_{13} angle and mass hierarchy have been considered. Four oscillation scenarios have been studied as possible “true” cases. Supernova scenarios I and II are tested.

Figure 21 shows the χ^2 value from the minimization as a function of the supernova parameters for a 100 kton detector, considering scenario I (left) and II (right) as “true” supernova parameters. We compare the results obtained fixing the mixing angle to $\sin^2 \theta_{13} = 10^{-3} \pm 10^{-4}$ and normal mass hierarchy with the case of leaving the mixing angle free. We have chosen the case where the effect of the neutrino mixing is largest, namely when the “true” oscillation parameters correspond to normal mass hierarchy and large mixing angle. For other oscillation parameters, in particular for small mixing, the effect is invisible.

We see that the expected accuracies are similar to the ones obtained constraining the

n.h.-L and n.h.-S (all parameters free)

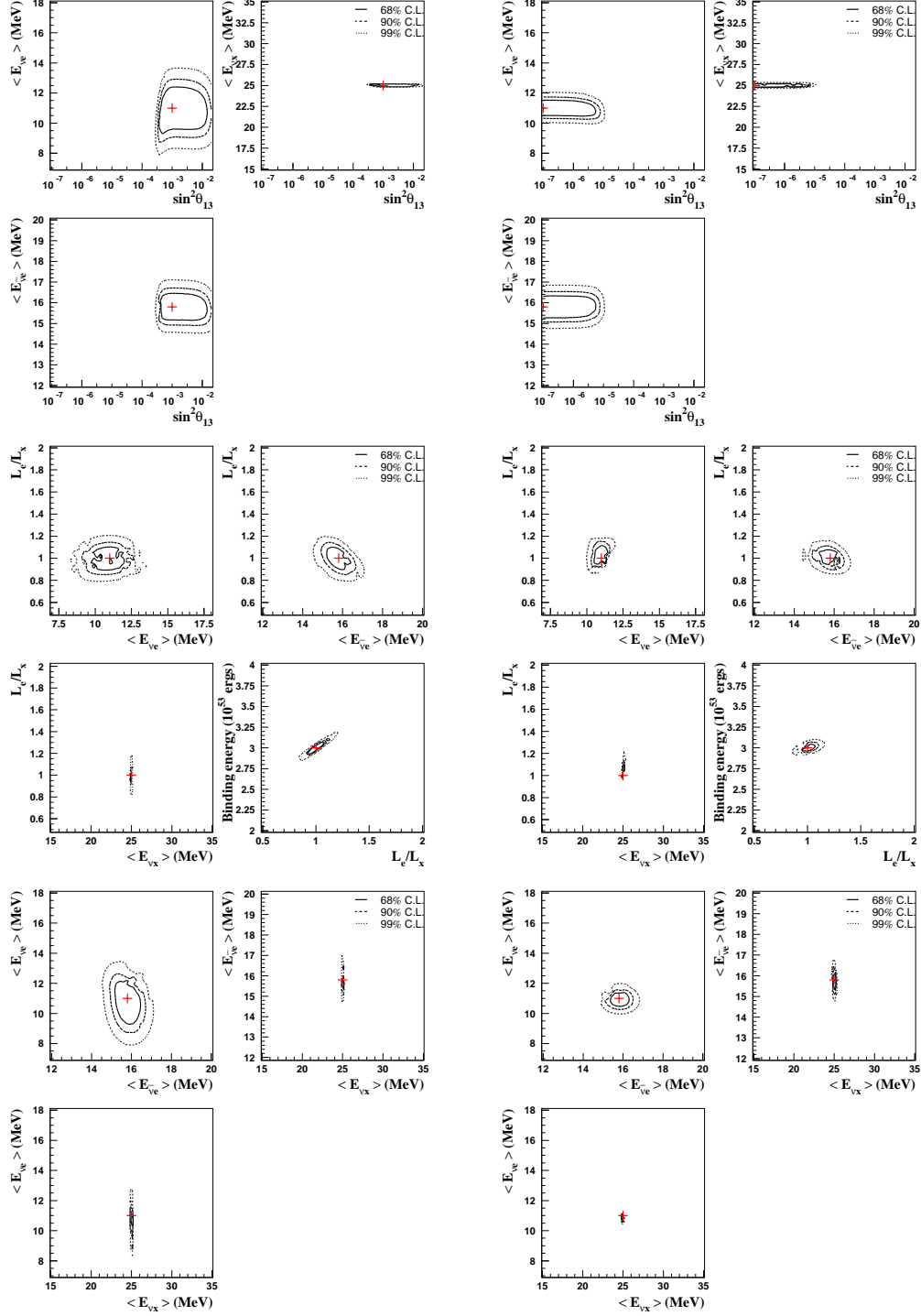


Figure 19: Correlation between oscillation and supernova parameters: 68%, 90% and 99% C.L. allowed regions for the supernova parameters without any assumption on the oscillation parameters for a 100 kton detector. The reference values correspond to the normal mass hierarchy, large (left) and small (right) θ_{13} mixing angle cases. Crosses indicate the value of the parameters for the best fits.

i.h.-L and i.h.-S (all parameters free)

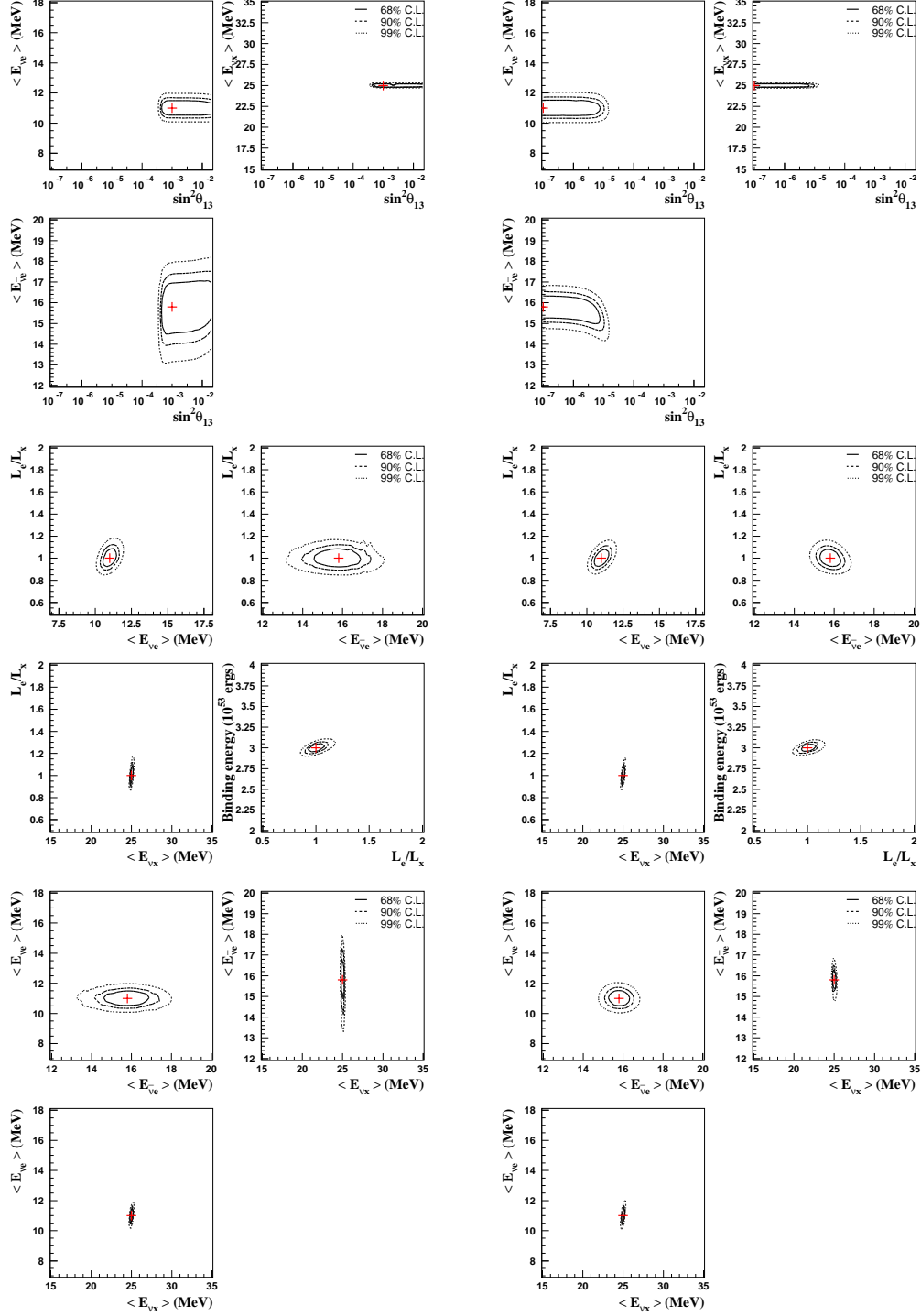


Figure 20: Correlation between oscillation and supernova parameters: 68%, 90% and 99% C.L. allowed regions for the supernova parameters without any assumption on the oscillation parameters for a 100 kton detector. The reference values correspond to the inverted mass hierarchy, large (left) and small (right) θ_{13} mixing angle cases. Crosses indicate the value of the parameters for the best fits.

mixing angle and the mass hierarchy, except for the $\langle E_{\nu_e} \rangle$ parameter and “true” oscillation case n.h.-L. In this scenario, the knowledge of the θ_{13} value improves the determination of the $\langle E_{\nu_e} \rangle$ energy from 17% to 14% for scenario I and from 21% to 9% for scenario II.

Hence, the observation of different channels which have different sensitivities to the neutrino flavors allows to decouple the supernova and neutrino oscillation physics, effectively allowing these two sectors to be studied independently. With the statistics provided by a 100 kton detector, a single supernova explosion would allow to determine the parameters of the supernova cooling phase quite precisely.

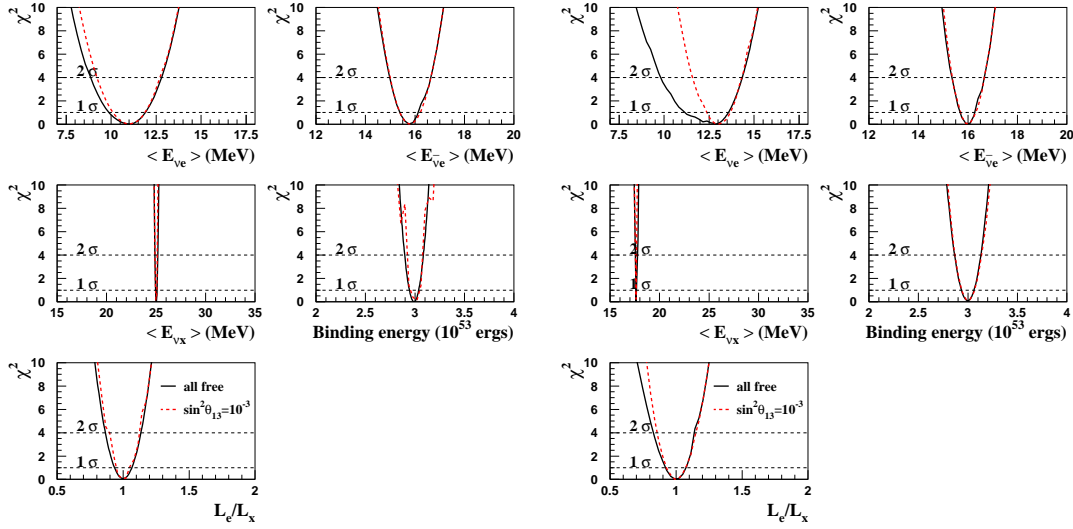


Figure 21: **Determination of the supernova parameters:** χ^2 value of the fit as a function of the supernova parameters for a 100 kton detector. We compare the results obtained fixing the angle to $\sin^2 \theta_{13} = 10^{-3} \pm 10^{-4}$ and normal mass hierarchy with the case of leaving all parameters free. The “true” supernova parameters correspond to scenario I (left) and to scenario II (right). The “true” oscillation parameters are normal mass hierarchy and large mixing angle.

8 Conclusions

In this paper we have investigated the capabilities of liquid argon TPC detectors to study and decouple supernova and neutrino oscillation physics in the event of the detection of a single core collapse supernova at an assumed distance of 10 kpc.

The neutrino physics was determined by the oscillation angle θ_{13} and the mass hierarchy. The supernova properties were summarized in five astrophysical parameters: the average energies of the neutrinos emitted from the supernova ($\langle E_{\nu_e} \rangle$, $\langle E_{\bar{\nu}_e} \rangle$, $\langle E_{\nu_x} \rangle$), the total binding energy (E_B) and the relative luminosities of the electron and non-electron flavor neutrinos (L_e/L_x). We considered two specific scenarios (I & II) in order to understand the effects of a hierarchical versus non-hierarchical distribution of energies of supernova neutrinos, since this issue is still debated. For the supernova scenario II, the differences between the average

energies of electron and non-electron neutrinos is of the order of 10%. This is an important issue since the interplay between hierarchy between neutrino flavors and neutrino mixing is expected to be a striking feature of matter enhanced oscillations in the supernova. In the case of degenerate neutrinos, the effect of oscillation is more difficult to observe. To contemplate two scenarios allowed us to address this in a quantitative way.

We have considered the four neutrino detection channels available in argon: elastic scattering on atomic electrons, charged-current interactions on argon (independently sensitive to ν_e and $\bar{\nu}_e$ neutrinos) and neutral-current interactions on argon.

In the first part of the work, we have studied the sensitivity to the θ_{13} and mass hierarchy parameters under the assumption of the supernova scenario I. For the true large mixing angle ($> 3 \times 10^{-4}$), a mass hierarchy identification is possible and lower limits on the θ_{13} value are set. We have shown that the detection of the NC process is important in this context. For small mixing angle ($< 2 \times 10^{-6}$), it is not possible to distinguish the mass hierarchy but upper limits on θ_{13} can be obtained. If the mixing angle is in an intermediate range ($2 \times 10^{-6} < \sin^2 \theta_{13} < 3 \times 10^{-4}$), measurements of its value are possible.

For the supernova scenario II, we found with the statistics provided by a 3 kton detector the possibility to determine the θ_{13} mixing angle is limited. More statistics, such as the one obtained with a 100 kton detector, will be mandatory to determine quantitatively the oscillation parameter.

In the second part of our study, we have studied the ability to determine the supernova parameters considering two different cases for the θ_{13} angle: (a) the angle has been determined by long-baseline experiments with $\approx 10\%$ precision, (b) an upper limit on the mixing angle has been set by long-baseline experiments. For a 3 (100) kton detector, the supernova parameters are measured with such accuracies: the total binding energy (E_B) has an error 20–30% (2–4%), the average energy of electron neutrinos $\langle E_{\nu_e} \rangle$ at the core is determined with an error 30–120% (5–14%), the average energy of electron antineutrinos $\langle E_{\bar{\nu}_e} \rangle$ at the core, with an error 30–80% (3–9%), the average energy of other (anti)neutrinos $\langle E_{\nu_x} \rangle$ at the core is determined with an error 3–23% ($< 1\%$), and the relative luminosities of the electron and non-electron flavor neutrinos L_e/L_x , with an error $> 100\%$ (10–40%).

In the last part of our study, we have considered the case where both supernova and oscillation parameters are free in the minimization. The precision with which the supernova parameters can be determined without knowledge on the neutrino mixing parameter is essentially the same as when information from terrestrial experiments would be available, except in the supernova scenario II and in large mixing angle case where the determination of the $\langle E_{\nu_e} \rangle$ energy profits largely from the terrestrial knowledge on θ_{13} .

In conclusion, the possibility provided by liquid Argon TPCs to observe elastic, charged and neutral current channels with different sensitivities to the neutrino flavors allows to disentangle the supernova and neutrino oscillation physics, allowing these two sectors to be effectively decoupled and studied independently. With the statistics provided by a 100 kton detector, a single supernova explosion would allow to determine the supernova cooling phase quite precisely. This is true even in the case that the energies of the neutrinos of different flavors are almost degenerate, as some recent supernova simulations indicate.

References

- [1] K. Hirata *et al.*, *Phys. Rev. D* **38** (1988) 448; *Phys. Rev. Lett.* **58** (1987) 1490.
R. Bionta *et al.*, *Phys. Rev. Lett.* **58** (1987) 1494.
- [2] Y. Fukuda, “Observation of supernova neutrino burst at Super-Kamiokande,” *Prepared for International Symposium on Origin of Matter and Evolution of Galaxies 2000, Tokyo, Japan, 19-21 Jan 2000*
- [3] N. W. Tanner and G. Doucas, “Supernova Detection By SNO,” *Prepared for 3rd NESTOR Workshop, Pylos, Greece, 19-21 Oct 1993*
- [4] S. Fukuda *et al.*, *Phys. Rev. Lett.* **86** (2001) 5656.
SNO Collaboration, *Phys. Rev. Lett.* **87** (2001) 071301.
Y. Fukuda *et al.*, *Phys. Rev. Lett.* **82** (1999) 2644.
KamLAND Collaboration, *Phys. Rev. Lett.* **90** (2003) 021802.
K2K Collaboration, *Phys. Rev. Lett.* **90** (2003) 041801.
- [5] M. Apollonio *et al.* [CHOOZ Collaboration], *Phys. Lett. B* **466** (1999) 415, [hep-ex/9907037](#). F. Boehm *et al.*, *Phys. Rev. D* **64** (2001) 112001, [hep-ex/0107009](#).
- [6] L. Wolfenstein, *Phys. Rev. D* **17** (1978) 2369. *Phys. Rev. D* **20** (1979) 2634.
S. P. Mikheyev and A. Yu. Smirnov, *Sov. J. Nucl. Phys.* **42** (1986) 913.
- [7] V. Barger, D. Marfatia and B.P. Wood, *Phys. Lett. B* **547** (2002) 37.
- [8] H. Minakata, H. Nunokawa, R. Tomas and J.W.F. Valle, *Phys. Lett. B* **542** (2002) 239.
- [9] C. Lunardini and A. Y. Smirnov, *Probing the neutrino mass hierarchy and the 13 -mixing with supernovae*, *J. Cosmol. Astropart. Phys.* **6** (2003) 009.
- [10] A. Bandyopadhyay, S. Choubey, S. Goswami and K. Kar, *Prospects of probing θ_{13} and neutrino mass hierarchy by supernova neutrinos in KamLAND*, [hep-ph/0312315](#).
- [11] I. Gil-Botella and A. Rubbia, *Oscillation effects on supernova neutrino rates and spectra and detection of the shock breakout in a liquid argon TPC*, *J. Cosmol. Astropart. Phys.* **10** (2003) 009, [hep-ph/0307244](#).
- [12] P. Aprili *et al.* [ICARUS Collaboration], “The ICARUS experiment: A second-generation proton decay experiment and neutrino observatory at the Gran Sasso laboratory. Cloning of T600 modules to reach the design sensitive mass. (Addendum),” LNGS-EXP 13/89 add.2/01, and CERN-SPSC-2002-027. All proposals are available at <http://www.cern.ch/icarus>.
- [13] D. B. Cline, F. Sergiampietri, J. G. Learned and K. McDonald, *LANNDD: A massive liquid argon detector for proton decay, supernova and solar neutrino studies, and a neutrino factory detector*, *Nucl. Instrum. Methods A* **503** (2003) 136, [astro-ph/0105442](#).
- [14] A. Rubbia, *Experiments for CP-violation: A giant liquid argon scintillation, Cerenkov and charge imaging experiment?*, [hep-ph/0402110](#). To appear in *Proceedings of the II International Workshop on Neutrino Oscillations in Venice, Italy*.

- [15] M. T. Keil, G. G. Raffelt and H. T. Janka, *Monte Carlo study of supernova neutrino spectra formation*, *Astrop. Phys. J.* **590** (2003) 971, [astro-ph/0208035](#).
G. G. Raffelt, M. T. Keil, R. Buras, H. T. Janka and M. Rampp, *Supernova neutrinos: Flavor-dependent fluxes and spectra*, [astro-ph/0303226](#).
- [16] K. Langanke, P. Vogel and E. Kolbe, *Phys. Rev. Lett.* **76** (1996) 2629.
- [17] A. S. Dighe and A. Y. Smirnov, *Phys. Rev. D* **62** (2000) 033007.
- [18] E. Kolbe, K. Langanke, G. Martínez Pinedo and P. Vogel, *Neutrino-nucleus reactions and nuclear structure*, *J. Phys. G: Nucl. Part. Phys.* **29** (2003) 2569.
- [19] F. James, MINUIT manual, CERN program libraries p. 43
- [20] M. Apollonio *et al.*, *Oscillation physics with a neutrino factory*, CERN-TH-2002-208, [hep-ph/0210192](#).
P. Huber, M. Lindner and W. Winter, *Superbeams versus neutrino factories*, *Nucl. Phys. B* **645** (2002) 3, [hep-ph/0204352](#).